Neoadjuvant enoblituzumab in localized prostate cancer: a single-arm, phase 2 trial

Eugene Shenderov [1,2] ✉, Angelo M. De Marzo [1,3,4], Tamara L. Lotan [1,3,4], Hao Wang [5], Sin Chan[1], Su Jin Lim[5], Hongkai Ji [6], Mohamad E. Allaf[4], Carolyn Chapman[1], Paul A. Moore[7], Francine Chen[7], Kristina Sorg[8], Andrew M. White[8], Sarah E. Church [8], Briana Hudson[8], Paul A. Fields [9], Shaohui Hu[10], Samuel R. Denmeade[1], Kenneth J. Pienta [1], Christian P. Pavlovich[4], Ashley E. Ross[11], Charles G. Drake[12], Drew M. Pardoll[1,2] & Emmanuel S. Antonarakis [1,2,13]

B7 homolog 3 (B7-H3; *CD276*), a tumor-associated antigen and possible immune checkpoint, is highly expressed in prostate cancer (PCa) and is associated with early recurrence and metastasis. Enoblituzumab is a humanized, Fc-engineered, B7-H3-targeting antibody that mediates antibody-dependent cellular cytotoxicity. In this phase 2, biomarker-rich neoadjuvant trial, 32 biological males with operable intermediate to high-risk localized PCa were enrolled to evaluate the safety, anti-tumor activity and immunogenicity of enoblituzumab when given before prostatectomy. The coprimary outcomes were safety and undetectable prostate-specific antigen (PSA) level (PSA_0) 1 year postprostatectomy, and the aim was to obtain an estimate of PSA_0 with reasonable precision. The primary safety endpoint was met with no notable unexpected surgical or medical complications, or surgical delay. Overall, 12% of patients experienced grade 3 adverse events and no grade 4 events occurred. The coprimary endpoint of the PSA_0 rate 1 year postprostatectomy was 66% (95% confidence interval 47–81%). The use of B7-H3–targeted immunotherapy in PCa is feasible and generally safe and preliminary data suggest potential clinical activity. The present study validates B7-H3 as a rational target for therapy development in PCa with larger studies planned. The ClinicalTrials.gov identifier is NCT02923180.

PCa is the second most common cause of cancer-related death in men[1]. The only modality with a potential for cure remains definitive local therapy, with either surgery or radiation therapy[2,3]. However, patients with high-risk features (Gleason-grade group 4–5 and/or PSA > 20 ng ml−1 and/or clinical stage T3 or T4) continue to have high relapse rates exceeding 70%[2,3]. It is increasingly recognized that patients with recurrence after primary local treatment are at greater risk of developing metastatic disease, which is responsible for most deaths

[1]Department of Oncology, Johns Hopkins School of Medicine, Baltimore, MD, USA. [2]The Bloomberg–Kimmel Institute for Cancer Immunotherapy, Johns Hopkins School of Medicine, Baltimore, MD, USA. [3]Department of Pathology, Johns Hopkins School of Medicine, Baltimore, MD, USA. [4]Department of Urology, Johns Hopkins School of Medicine, Baltimore, MD, USA. [5]Department of Oncology Biostatistics and Bioinformatics, Johns Hopkins School of Medicine, Baltimore, MD, USA. [6]Department of Biostatistics, Johns Hopkins Bloomberg School of Public Health, Baltimore, MD, USA. [7]MacroGenics, Inc., Rockville, MD, USA. [8]NanoString Technologies Inc., Seattle, WA, USA. [9]Adaptive Biotechnologies, Seattle, WA, USA. [10]CDI Labs, Baltimore, MD, USA. [11]Department of Urology, Northwestern University Feinberg School of Medicine, Chicago, IL, USA. [12]Immuno-Oncology, Janssen, Horsham, PA, USA. [13]Present address: University of Minnesota Masonic Cancer Center, Minneapolis, MN, USA. ✉e-mail: Eugene.Shenderov@jhmi.edu

from prostate cancer[4]. Thus, safe and effective neoadjuvant and/or adjuvant therapies for such high-risk patients are urgently needed.

Improvements over the past 20 years in understanding and the ability to manipulate the immune system have resulted in unprecedented advances in the treatment of multiple malignancies, including melanoma, and lung and colorectal cancers[5]. Immunotherapy can potentially promote systemic anti-tumor immune responses that may control distant micrometastasis, together with long-lived anti-tumor immunity[6]. The US Food and Drug Administration (FDA) in 2010 approved a therapeutic cancer vaccine for patients with asymptomatic or minimally symptomatic, metastatic, castrate-resistant prostate cancer (mCRPC), sipuleucel-T[7]. Recent data mostly involve immune-checkpoint blockade strategies using CTLA-4 or programmed cell death protein 1 (PD-1)/programmed cell death ligand 1 (PD-L1) antibodies, but, despite some promising early results[8], those therapies have yielded limited overall survival benefit in PCa (even when used in combination)[9,10], partly due to the low prevalence of PD-L1 expression in PCa, prompting the search for alternative immunological approaches in this disease.

In contrast to PD-L1, B7 homolog 3 (B7-H3, PD-L3, *CD276*) is highly expressed in PCa. B7-H3 is a member of the B7 superfamily of coregulatory molecules, which includes PD-L1 (B7-H1) and PD-L2 (B7-DC)[11]. A series of large radical prostatectomy cases showed that, compared with benign prostatic tissue, PCa demonstrated substantially higher expression of *CD276* messenger RNA and, although PD-L1, PD-L2 and B7-H4 were not highly expressed in PCa, B7-H3 mRNA expression was within the top fifth of genes expressed, making this a potentially appealing immunotherapeutic target specifically for PCa[12]. It is possible to target B7-H3-expressing cells in humans with multiple agents in clinical development, including enoblituzumab (MacroGenics, Inc.), a humanized, Fc-engineered, monoclonal antibody binding B7-H3 with high affinity and engineered to mediate antibody-dependent cellular cytotoxicity (ADCC)[13]. ADCC is known to be a central mechanism of activity for several monoclonal antibodies, including rituximab and trastuzumab[14].

We hypothesized that B7-H3-targeted antibodies with ADCC activity might improve outcomes in men with high-risk prostate cancer undergoing curative-intent local therapy, by inducing local tumor-directed immune responses that resulted in systemic immune responses able to eliminate micrometastatic disease. In the present study, we report results from an investigator-initiated, single-arm, phase 2, biomarker-rich, neoadjuvant trial in men with operable, localized, intermediate to high-risk PCa treated with 6 weekly infusions of enoblituzumab therapy before radical prostatectomy. Primary endpoints were safety and anti-tumor activity based on undetectable PSA 1 year postprostatectomy (PSA$_0$), with adjuvant or salvage therapies considered as progression events. Secondary outcomes were tumor microenvironment (TME) immune changes pre- and posttreatment and Gleason-grade group changes from biopsy to prostatectomy. Finally, to identify determinants of anti-tumor potency and/or immune resistance, we investigated tumor and peripheral blood T cell clonal expansion using T cell receptor (TCR)-sequencing, tumor genomics and protein arrays to assess development of tumor-associated antigen (TAA)-specific antibodies, and conducted comprehensive transcriptomic and proteomic spatial profiling of the TME before and after enoblituzumab treatment.

Results

Patient characteristics

From 14 February 2017 to 10 June 2019, 32 patients were enrolled. In total, 75 patients were assessed for eligibility and 43 were excluded (Fig. 1a). One patient only received five out of six doses of study drug due to a grade 2 infusion reaction. Baseline characteristics for all patients are summarized in Table 1. None of the patients had received previous local or systemic therapy. The median age of participants was 64 years (range 48–74 years), 97% had Eastern Cooperative Oncology Group (ECOG) performance status of 0, 47% had a PSA >10 ng ml−1 at diagnosis, 50%
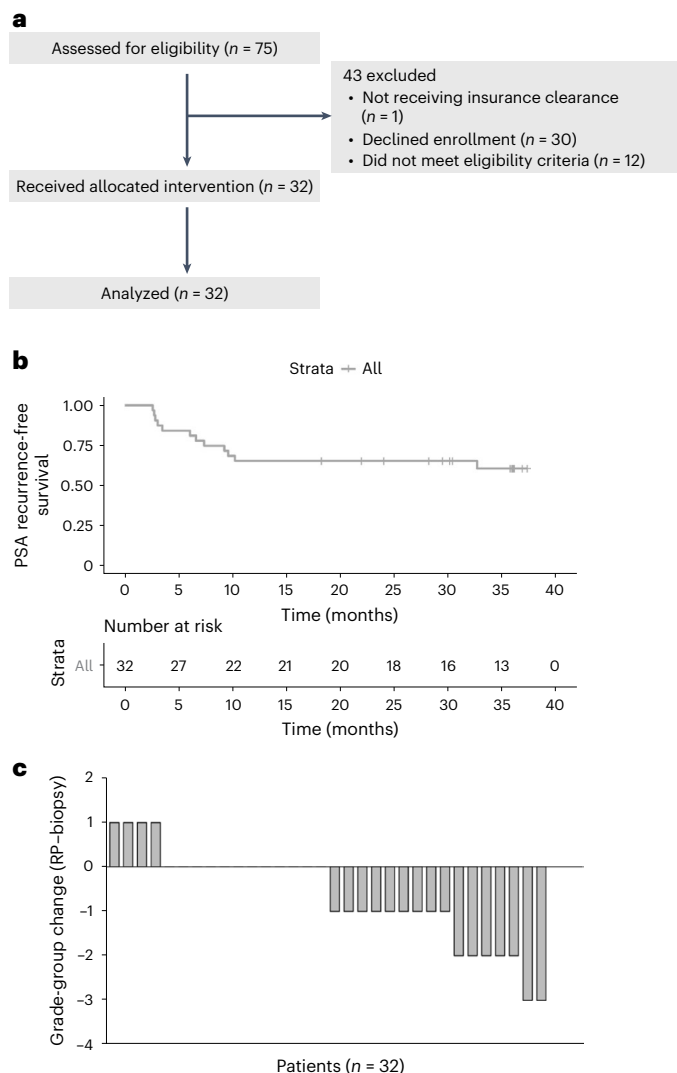
Fig. 1 | Patient consort diagram and efficacy outcomes in the neoadjuvant treatment of patients with PCa using enoblituzumab. a, Patient consort diagram. **b**, Kaplan–Meier curve showing median time to PSA recurrence (PSA ≥ 0.2 ng ml−1) after radical prostatectomy. The 95% CIs for point estimates are shown in gray shading. **c**, Waterfall plot of Gleason-grade group change from biopsy to radical prostatectomy (RP).

had Gleason-grade group 5 at biopsy, and 97% (all but one) were classified as having high-risk PCa and 72% as having very-high-risk (VHR) PCa.

Clinical outcomes. The median follow-up from radical prostatectomy at the time of data cut-off (20 January 2022) was 30 months (range 3–37 months). All 32 enrolled patients were evaluable for the coprimary endpoints of safety and efficacy defined as undetectable PSA at 12 months after radical prostatectomy. A clinical biospecimen collection schema is outlined in Extended Data Fig. 1. Of 32 patients, 21 (66%, 95% confidence interval (CI) 47–81%) had an undetectable PSA level 12 months after prostatectomy (Supplementary Table 1) and the median PSA recurrence-free survival time had not been reached after 30 months of follow-up (95% CI 32.7, not reached (NR); Fig. 1b). The present study was not powered for this endpoint and it was obtained as an estimate of PSA$_0$ with reasonable precision.

Safety

The coprimary trial endpoint, around which the trial was designed, was safety and feasibility of administering enoblituzumab therapy before radical prostatectomy. Treatment-related adverse events (AEs)

Table 1 | Baseline patient demographics and clinical characteristics

	Overall
	(n=32)
Age (years)	
Mean (s.d.)	63.1 (6.95)
Median (minimum, maximum)	64.0 (48.0, 74.0)
Age (years)	
65+, n (%)	15 (46.9)
<65, n (%)	17 (53.1)
Race, n (%)	
White	30 (93.8)
Black	1 (3.1)
Asian	1 (3.1)
Smoking history, n (%)	
Yes	9 (28.1)
No	23 (71.9)
Family prostate cancer history, n (%)	
Yes	7 (21.9)
No	25 (78.1)
PSA>10 ng ml−1 at diagnosis, n (%)	
Yes	15 (46.9)
No	17 (53.1)
Time from study entry to prostatectomy (weeks)	
Mean (s.d.)	7.00 (0.392)
Median (minimum, maximum)	6.86 [6.57, 8.29]
ECOG, n (%)	
0	31 (96.9)
1	1 (3.1)
Body mass index (kg m^2), n (%)	
Normal (18.5–24.9)	6 (18.8)
Overweight (25.0–29.9)	14 (43.8)
Obese (30.0+)	12 (37.5)
Gleason-grade group at biopsy, n (%)	
3	5 (15.6)
4	11 (34.4)
5	16 (50.0)
Previous therapy, n (%)	
No	32 (100)
T stage, n (%)	
pT2	8.0 (25.0)
pT3a	16.0 (50.0)
pT3b	8.0 (25.0)
Patients with high-risk localized PCa[a]	
Yes, n (%)	31.0 (96.9)
No, n (%)	1 (3.1)
Patients with VHR localized PCa[b]	
Yes, n (%)	23.0 (71.9)
No, n (%)	9 (28.1)

[a]High-risk group defined by National Comprehensive Cancer Network (NCCN) criteria as Gleason ≥8 or PSA>20 ng ml−1 or clinical T3 stage or higher. [b]VHR group defined as having at least one of the following: cT3b–cT4, primary Gleason pattern 5 on biopsy, >4 biopsy cores with a Gleason sum of 8–10 or 2–3 NCCN high-risk features.

are summarized in Table 2. Overall, enoblituzumab was well tolerated. Six grade 3 AEs occurred in 4 of 32 patients (12%), with no grade 4 events noted. One patient experienced an infusion-related reaction associated with hypotension, another with asymptomatic amylase/lipase elevation, another had a maculopapular rash and another experienced perimyocarditis with pericardial effusion. The perimyocarditis occurred 1 month after completion of the study drug, did not negatively affect the radical prostatectomy and resolved with oral corticosteroid therapy. Pneumonitis, hepatitis, hypophysitis, thyroiditis and colitis were not observed. Radical prostatectomy was achieved successfully in all enrolled patients with no notable unexpected surgical or medical complications, or surgical delay. There were no treatment-related deaths and all 32 patients were alive at data cut-off.

Preplanned secondary endpoint pathological assessments were next undertaken to contextualize the safety and PSA_0 coprimary endpoints. Pathology outcomes at radical prostatectomy are summarized in Extended Data Table 1. The secondary endpoint of enoblituzumab intraprostatic distribution in treated patients revealed that enoblituzumab was confirmed to penetrate the prostate and bind B7-H3 in 28 of 32 (88%) patient prostatectomy frozen sections (Extended Data Fig. 2). In four cases, enoblituzumab binding was not detected. For two of the four patients, there were insufficient tumor cells in the biopsy material either to score B7-H3 or to detect enoblituzumab binding. For two additional patients, we did observe B7-H3 tumor expression, but no detectable enoblituzumab, possibly due to the sensitivity of the anti-enoblituzumab assay. No association between B7-H3 prostatectomy expression level and response was noted. At prostatectomy, 25% of patients had seminal vesicle invasion, 6% had lymphovascular invasion, 59% had extraprostatic extension, 31% had positive surgical margins and 13% were found to have N1 disease. None of the 32 men achieved the secondary endpoint of complete pathological response and there were no clear histopathological signs of tumor regression. Prespecified secondary analysis of Gleason-grade groups showed that the grades found in carcinomas from 16 patients (50%) at prostatectomy were lower than on corresponding biopsy and in seven of the tumors (22%) there was a difference of two or more groups lower (Fig. 1c).

Exploratory analysis of early treatment progression revealed that 26 of 32 patients (81%, 95% CI 64–93%) had an undetectable PSA (defined as <0.1 ng ml−1) at 3 months after radical prostatectomy (Supplementary Table 2). An exploratory McNemar test comparison of the proportion of Gleason-grade group downgrade between one-to-one matched treated and matched control (matched by Gleason-grade group, stage, margins, block age (within 2 years), age (within 2 years) and self-reported race) prostatectomy cases revealed a statistically significant association between enoblituzumab treatment and net-grade group decrease (P = 0.016; Supplementary Table 3 and Extended Data Fig. 3). Furthermore, we were able to retrospectively review all paired biopsy and radical prostatectomy cases from our institution over the time period 2015–2022, with a total of 1,631 cases identified showing 588 cases downgraded by at least one grade group at radical prostatectomy, compared with biopsy (Supplementary Table 4). This equated to a 36% downgrading rate versus 50% seen in the present study.

T cell repertoire compartment dynamics and clinical outcomes

In exploratory analyses, we next investigated whether clinical outcomes were associated with an anti-tumor immune response as evidenced through T cell repertoire dynamics intratumorally or in the peripheral blood. TCR-seq was performed successfully on posttreatment prostatectomy of fresh frozen tumor areas, as well as pre- and posttreatment blood samples for 30 of 32 patients. We observed that all patients (7 of 7), whose peripherally expanded clones were also 100% present intratumorally, demonstrated the coprimary outcome of PSA_0 at 1 year (Fig. 2a, Extended Data Fig. 4 and Supplementary Table 5). Furthermore,

Table 2 | All treatment-related AEs by type and grade

AE CTCAE terminology	All grade AEs, n (%)	Grade 1, n (%)	Grade 2, n (%)	Grade 3, n (%)	Grade 4, n (%)
Total independent patients		31/32 (97)	12/32 (38)	4/32 (12)	0/32 (0)
Fatigue	23 (72)	22 (69)	1 (3)	0 (0)	0 (0)
Neurological (headache, dizziness, paresthesia)	14 (44)	13 (41)	1 (3)	0 (0)	0 (0)
Flu-like/cold symptoms	13 (41)	12 (38)	1 (3)	0 (0)	0 (0)
Gastrointestinal (nausea, vomiting, anorexia, constipation, weight gain)	12 (38)	10 (31)	2 (6)	0 (0)	0 (0)
Upper respiratory infection, cough, nasal congestion, chills, fever, sore throat	12 (38)	9 (28)	3 (9)	0 (0)	0 (0)
Infusion-related reaction	7 (22)	1 (3)	5 (16)	1 (3)	0 (0)
Arthralgia/Myalgia	6 (19)	5 (16)	1 (3)	0 (0)	0 (0)
Amylase/Lipase increased	3 (9)	1 (3)	1 (3)	1 (3)	0 (0)
Rash, maculopapular	3 (9)	2 (6)	0 (0)	1 (3)	0 (0)
Anemia	2 (6)	1 (3)	1 (3)	0 (0)	0 (0)
Dermatitis/Pruritus	2 (6)	2 (6)	0 (0)	0 (0)	0 (0)
Edema lower extremities	2 (6)	2 (6)	0 (0)	0 (0)	0 (0)
Hypotension	2 (6)	1 (3)	0 (0)	1 (3)	0 (0)
Skin subcutaneous tissue disorder (bruising, intravenous infiltration, flushing)	2 (6)	2 (6)	0 (0)	0 (0)	0 (0)
Bilirubin increase	1 (3)	1 (3)	0 (0)	0 (0)	0 (0)
CD4 lymphocytes decreased	1 (3)	1 (3)	0 (0)	0 (0)	0 (0)
Diarrhea/Colitis	1 (3)	1 (3)	0 (0)	0 (0)	0 (0)
Dry mouth	1 (3)	1 (3)	0 (0)	0 (0)	0 (0)
Dysgeusia	1 (3)	1 (3)	0 (0)	0 (0)	0 (0)
Electrolyte change (hypocalcemia, hypercalcemia, hyponatremia, hypokalemia)	1 (3)	1 (3)	0 (0)	0 (0)	0 (0)
Myocarditis/Pericarditis	1 (3)	0 (0)	0 (0)	1 (3)	0 (0)
Pericardial effusion	1 (3)	0 (0)	0 (0)	1 (3)	0 (0)
Platelet count decreased	1 (3)	1 (3)	0 (0)	0 (0)	0 (0)
Vascular disorders	1 (3)	1 (3)	0 (0)	0 (0)	0 (0)

all of these patients exhibited a limited amount of clonal expansion, <50 clones. These 7 individuals had 58 expanded clones in total and only 1 of these clones had a match—for cytomegalovirus—in a curated database, VDJdb, of TCR sequences with known antigen specificities including viral antigens (Supplementary Table 6). We did not observe similar correlation for post hoc analysis of men with the greatest Gleason declines, downgrade ≥2 (Fig. 2b).

Spatial TME transcriptomic and proteomic characterization
In further preplanned exploratory analysis, we next examined the TME utilizing protein-based, digital spatial profiling to assess how enoblituzumab impacted T cell activation and effector function, myeloid cell infiltration and markers of immune activation and suppression (Fig. 3a). Matched-patient pretreatment biopsies (n = 28 patients and 199 regions) and posttreatment prostatectomies (n = 31 patients and 264 regions) were evaluated (Fig. 3b). Evidence of broad immune-stimulatory activity, including augmented markers of cytotoxicity (increased granzyme B (GZMB), P = 0.004 and OX40L, P = 0.003), was observed after treatment (Fig. 3c and Supplementary Table 7). Markers of granulocyte (CD66B, P = 0.0003), leukocyte (CD45, P = 0.001), effector T cells (CD8, P = 0.004) and monocytic antigen-presenting cells (human leukocyte antigen (HLA)-DR, P = 0.0007; CD163, P = 0.0006) were also upregulated. A 1.8-fold increase in tumor CD8+ cytotoxic T cells was noted between patient posttreatment prostatectomies compared

with pretreatment biopsies (Fig. 3c and Supplementary Table 7). Inhibitory markers associated with adaptive immunosuppressive mechanisms, such as PD-L1, FoxP3 (forkhead box P3) and B7-H3 (the target of enoblituzumab) were upregulated as well.

To determine whether the observed protein measurement changes correlated with their corresponding mRNA levels, differential gene expression analysis was performed on normalized NanoString IO360 data utilizing bulk RNA from enoblituzumab-treated patient prostatectomies and untreated control prostatectomies that were on-to-one matched (Gleason-grade group, stage, margins, block age (within 2 years), age (within 2 years) and self-reported race). This analysis showed increased markers of immune inflammation in enoblituzumab-treated prostatectomies (including CXCL16, CSF1R, HLA-DPB1, IFNAR1, IL-18 and HLA-DRA) compared with increased markers of immunosuppression and aggressive PCa in untreated controls (including PVR and WNT5B) (Extended Data Fig. 5).

Stratification by the coprimary clinical endpoint of responders (PSA₀) and nonresponders (PSA recurrent) at 1 year revealed more pronounced protein expression changes for responders (Fig. 3d) versus nonresponders (Fig. 3e), although the results were not statistically significant (Extended Data Fig. 6a and Supplementary Table 8). B7-H3 expression level itself, either pretreatment (biopsy) or radical prostatectomy posttreatment, did not associate with clinical outcome of PSA₀ responder or nonresponder at 1 year (Supplementary Table 9).
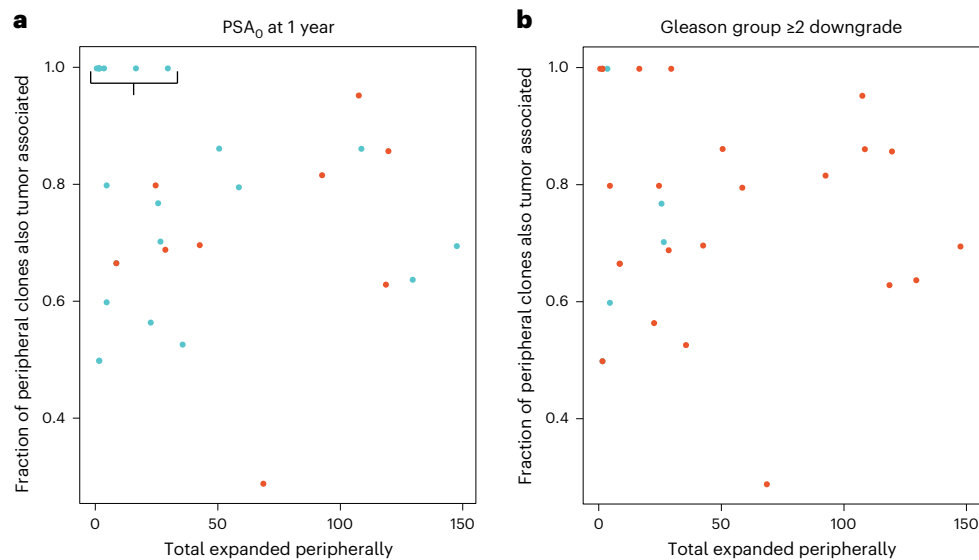
Fig. 2 | TCR repertoire dynamics in peripheral blood and tumor, and association with anti-tumor response. a,b, Number of clones expanded peripherally versus fraction of peripheral clones expanded and detected intratumorally in evaluable samples from $n = 30$ patients ($n = 30$ tissue and $n = 30$ blood samples) by PSA_0 at the 1-year clinical response (**a**) and Gleason-grade group downgrade ≥2 (**b**). Each point on the scatter plots represents a patient. Blue dots indicate responders for a given outcome and red dots the nonresponders. The bracket indicates all patients (7 of 7) who demonstrated PSA_0 at 1 year and whose peripherally expanded T cell clones were 100% matched to their intratumorally associated T cell clones.

Stratification by patients with Gleason-grade group change (analyzed for decline <2 versus stringently as decline ≥2) showed upregulated immune protein expression that was particularly notable for individuals with Gleason-grade group decline ≥2, but the results were not statistically significant (Fig. 3f,g, Extended Data Fig. 6b and Supplementary Table 10).

Exploratory treatment-induced antibody reactivity assessment

We attempted to extend our TME cellular analysis to determine the breadth of treatment-induced antibody reactivity via on-target antibody responses or possibly off-target autoantibody formation. HuProt v.4.0, human, full-length proteome microarrays (containing >21,000 human proteins and protein isoforms covering >80% of the human proteome) were utilized to quantify antigen spread to on-target or off-target antigens in participants immediately before prostatectomy or 30 days postprostatectomy compared with baseline for immunoglobulin (Ig)G and IgM across all 32 trial patients. One IgG candidate, C1R, was increased after enoblituzumab treatment before prostatectomy (day or D50) and 30 days postprostatectomy. A single IgM candidate, PRB1, was identified between biopsy and 30 days postprostatectomy (Extended Data Fig. 7).

Exploratory cytokine, chemokine and soluble factor analysis

Changes between baseline and pre-prostatectomy (D50) blood samples for 18 soluble proteins are shown in Fig. 4. Soluble B7-H3 could be evaluated only at baseline due to assay interference posttreatment, with enoblituzumab binding to soluble B7-H3. Levels of interleukin (IL)-2 ($P = 0.05$), IL-36b ($P = 0.014$), IL-17 ($P = 0.009$) and soluble 4-1BB (CD137) ($P < 0.001$) were increased, whereas levels of IL-15 ($P < 0.001$) and IL-6 ($P = 0.02$) were decreased posttreatment.

Outlier analysis examining the lowest tertile versus the middle and upper tertiles for each factor at baseline before enoblituzumab treatment was utilized as a possible prognostic signature to enrich for possible responders versus nonresponders, according to patients with Gleason-grade group decline of ≥2 or PSA_0 response at 1 year (Extended Data Fig. 8). For each analyte, outcomes were compared for patients in the lowest tertile versus the middle and upper tertiles, with the

number of patients achieving an outcome summarized in Extended Data Fig. 8a,d, unadjusted odds ratios in Extended Data Fig. 8b,e and adjusted odds ratio (with adjustment for patient age) in Extended Data Fig. 8c,f. No statistically significant associations were noted for Gleason changes or PSA_0 outcomes.

Genomic alterations and clinical outcomes

Whole-exome DNA-sequencing (DNA-seq; 31 of 32 successful) of tumor from prostatectomy specimens was performed as summarized in Supplementary Tables 11 and 12. Mismatch repair deficiency was detected in one patient harboring loss of MLH1 and PSM2 proteins, but without microsatellite instability (MSI) or hypermutation on DNA-seq. Median tumor mutational load (TMB) was 0.5 (range, 0.1–4.5) mutations per Mb. Of 32 patients, 5 (15.6%) harbored potentially deleterious somatic mutations in at least one homologous recombination repair (HRR) gene. Post hoc analysis of PSA_0 response at 12 months after prostatectomy did not significantly associate with any genomic mutational groups, including HRR status or TMB categories (Supplementary Table 12). Time to PSA recurrence after radical prostatectomy also did not differ statistically by mutational group (Extended Data Fig. 9).

Discussion

The present study evaluated the safety and clinical activity of B7-H3-targeted, enoblituzumab monoclonal antibody immunotherapy in patients with aggressive, clinically localized PCa in a window-of-opportunity neoadjuvant setting. Overall, treatment was well tolerated, did not reveal unexpected surgical complications or delays to prostatectomy and the study met its primary safety endpoint. The coprimary endpoint of undetectable PSA (PSA < 0.1 ng ml−1) at 12 months after radical prostatectomy (PSA_0) was observed in 66% of patients at 30 months of median follow-up without any preoperative or postoperative androgen deprivation therapy (ADT) or radiation therapy. Trial progression was defined as PSA ≥ 0.2 ng ml−1 (confirmed by a second PSA of the same level or higher) or start of salvage or adjuvant therapy when clinically indicated, whichever occurred first. Median time to PSA recurrence was not reached after 30 months of median follow-up. The statistical design for the coprimary endpoint of PSA_0 at 12 months was descriptive, with the goal to estimate the PSA_0 rate at 12 months

rather than hypothesis testing—the aim being to obtain a reasonably precise estimate of the PSA_0 for future randomized trial design.

To date, 203 patients (179 adult and 24 children) across a range of tumor types—head and neck squamous cell carcinoma, nonsmall-cell lung cancer, clear-cell renal carcinoma, triple-negative breast cancer, bladder and prostate cancer and melanoma—have received enoblituzumab monotherapy in phase 1 trials at doses up to 15 mg kg−1 (the dose given in the present study), with overall toxicities matching what we observed here (NCT01391143 and NCT02982941). The observed result compares favorably with historical expectations of high-risk PCa outcomes postprostatectomy (12-month PSA_0 rate of 60%), where 11.5–29% of men received presurgical ADT, 22–34% received postoperative radiation therapy and 19–38% received postoperative ADT[3]. Furthermore, the outcome appeared to at least match recent results from a population of roughly similar patients at our institution treated with neoadjuvant degarelix monotherapy before radical prostatectomy (12-month PSA_0 rate of 55%, control arm of trial in ref. 15. Preplanned secondary endpoint analysis of Gleason-grade group declines from biopsy to prostatectomy likewise appeared to exceed one-to-one matched control patient samples and the results from a 42-patient, neoadjuvant, sipuleucel-T (Sip-T) therapeutic vaccine trial[16]. Furthermore, the observed Gleason-grade group declines in the trial were a greater percentage compared with those observed in a retrospective analysis of all paired biopsy and radical prostatectomy cases from our institution over the time period 2015–2022, but, as patient characteristics were not matched between these populations, a planned, larger, randomized trial already in the development stages is required to corroborate or refute the findings herein.

The primary mechanism of action for enoblituzumab is believed to be ADCC, because enoblituzumab comprises an engineered human IgG1 Fc domain that imparts increased affinity for human-activating Fcγ receptor (FcγR) IIIA (CD16A) and decreased affinity for the human inhibitory FcγRIIB (CD32B)[13]. This mode of action is shared with FDA-approved monoclonal antibodies, including rituximab and trastuzumab[17], although enoblituzumab additionally mediates allotype-independent, enhanced ADCC similar to that of glycoengineered antibodies[18]. Enoblituzumab may also induce anti-tumor activity through enhancement of cytotoxic lymphocyte function by reduction of negative immunoregulatory signals through blocking the B7-H3 molecule on tumor cells[19,20], although the blocking activity of enoblituzumab is unknown because the putative B7-H3 receptor has not been elucidated. In contrast to PD-L1, B7-H3 expression is not interferon (IFN)-γ inducible, suggesting that PD-L1 and B7-H3 checkpoints might have distinct immune niches. Furthermore, B7-H3 has features of being a tumor-associated antigen in PCa with increased androgen receptor (AR) promoter/enhancer occupancy specifically in PCa and CRPC compared with normal prostate tissue[21]. Therefore, we hypothesized that B7-H3-targeted immunotherapy might improve outcomes in men with high-risk PCa undergoing curative-intent local therapy by inducing an immune response that can eliminate micrometastatic disease and/or deplete the most aggressive, highest-expressing B7-H3 PCa cells within the tumor. Clinical outcomes of the PSA recurrence rate at 1 year after prostatectomy, as well as Gleason-grade group declines before prostatectomy after 6 weeks of enoblituzumab treatment, appear to support this hypothesis.

The neoadjuvant biomarker-rich design of this trial and the absence of concurrent hormonal therapy allowed us to assess the systemic immune response in peripheral blood and the local TME response induced by enoblituzumab. Using TCR analysis to track clonal sharing and dynamics between the peripheral blood and intratumoral TME as a barcode, we observed a positive association between patients with the primary clinical endpoint of PSA_0 at 1 year and patients whose peripheral expanded clones were 100% present among their intratumoral clones, demonstrating focused clonal expansion (<50 clones), potentially toward tumor-specific antigens. No confounding relationship was observed between peripheral blood or tumoral total T cell numbers or total unique T cell clonotypes, and identification of fraction of peripherally expanded, tumor-associated T cell clones. This expands and adds to previous data showing that nonsmall-cell lung cancer and melanoma improved immunotherapy outcomes correlating with increased TCR clonality (decreased diversity) after immune-checkpoint blockade, potentially also due to a skewed response toward tumor-specific antigens[22,23]. However, it remains to be determined whether the repertoire skewing is due to either expansion of TAA or neoantigen-specific responses.

The presence of intratumoral, peripherally expanded T cell clones led us to comprehensively profile the pretreatment and posttreatment TME to identify potential immune response mechanisms underlying the observed clinical outcomes. Initially, we analyzed fresh frozen posttreatment prostatectomy tissue to assess whether the B7-H3 H-score revealed a level associated with response; however, no association between B7-H3 prostatectomy expression level and response was noted. Furthermore, spatial profiling analysis of >35 different proteins, including B7-H3, in the pre- and posttreatment TME of the 32 trial patients (spanning a combined 463 regions of interest (ROIs)) utilizing formalin-fixed, paraffin-embedded (FFPE) areas also did not reveal a B7-H3 level of expression correlating with the response, indicating that additional factors needed to be considered. Spatial profiling did indicate increased infiltration of CD8+ T cells, as well as granulocytic and myeloid cells, and upregulation of multiple immune activation and immunosuppressive markers, including PD-1/PD-L1, consistent with an inflammatory or 'hot' TME. Indeed, the 1.8-fold increase in tumor CD8+ cytotoxic T cells seen is at least equivalent to the CD8 recruitment into the TME after neoadjuvant Sip-T administration[16], with Sip-T being the first (and only) FDA-approved therapeutic vaccine in oncology, targeting prostatic acid phosphatase, which was approved in 2010 for patients with asymptomatic or minimally symptomatic mCRPC[7]. Generally, PCa has been shown to be poorly infiltrated by T cells, that is, immunologically 'cold', with low PD-L1 expression[24,25] and this probably partially explains why immune-checkpoint blockade using single-agent CTLA-4 or PD-1/PD-L1 antibodies has yielded minimal efficacy in PCa[26,27] with no PCa-specific FDA approvals of immune-checkpoint therapies to date.

Our exploratory data indicate that high levels of B7-H3 expression on PCa cells, combined with enhanced ADCC mediated by enoblituzumab, supported recruitment of resident myeloid and circulating granulocytic cells into the tumor thereby promoting, tumor-specific inflammation and apoptosis driving T cell recruitment, as suggested

Fig. 3 | Digital spatial profiling of the TME in pretreatment biopsies and posttreatment prostatectomies stratified by clinical outcomes.
a, Immunofluorescent staining of pretreatment (biopsy) and posttreatment (radical prostatectomy) tissue to select ROIs for DSP. Matched-patient pretreatment biopsies (n = 28 patients and 199 tumor regions) and posttreatment prostatectomies (n = 31 patients and 264 tumor regions) were evaluated. Tumor cells were identified with CK8/18, CD3 for T cells, CD68 for myeloid cells and Cyto83 for DNA content analysis. Two illustrative ROIs are depicted. **b**, Heatmap showing the relative quantification of 34 proteins detected in tumor ROIs in biopsy (pretreatment) and radical prostatectomy (posttreatment) specimens. **c**, Volcano plot overview of fold-changes (FC) in protein expression in tumor ROIs between pretreatment biopsy and posttreatment prostatectomy. **d**–**g**, Volcano plot overview of tumor region protein expression change for patients with PSA_0 at 1 year after prostatectomy (**d**) or PSA recurrence prior to 1 year (**e**), and protein expression change for patients who had Gleason-grade group downgrade ≥−2 from biopsy to prostatectomy (**f**) or <−2 (**g**). Proteins that remain significant after the Benjamini–Hochberg adjustment (P_{adj} < 0.01) are blue.

by GZMB upregulation associated with Gleason-grade group declines. Differential gene expression analysis between one-to-one matched, enoblituzumab-treated prostatectomies and untreated control prostatectomies further supported the emerging observation that the TME post-enoblituzumab is inflamed. Observed were indications of effector T cell function leading to compensatory adaptive upregulation
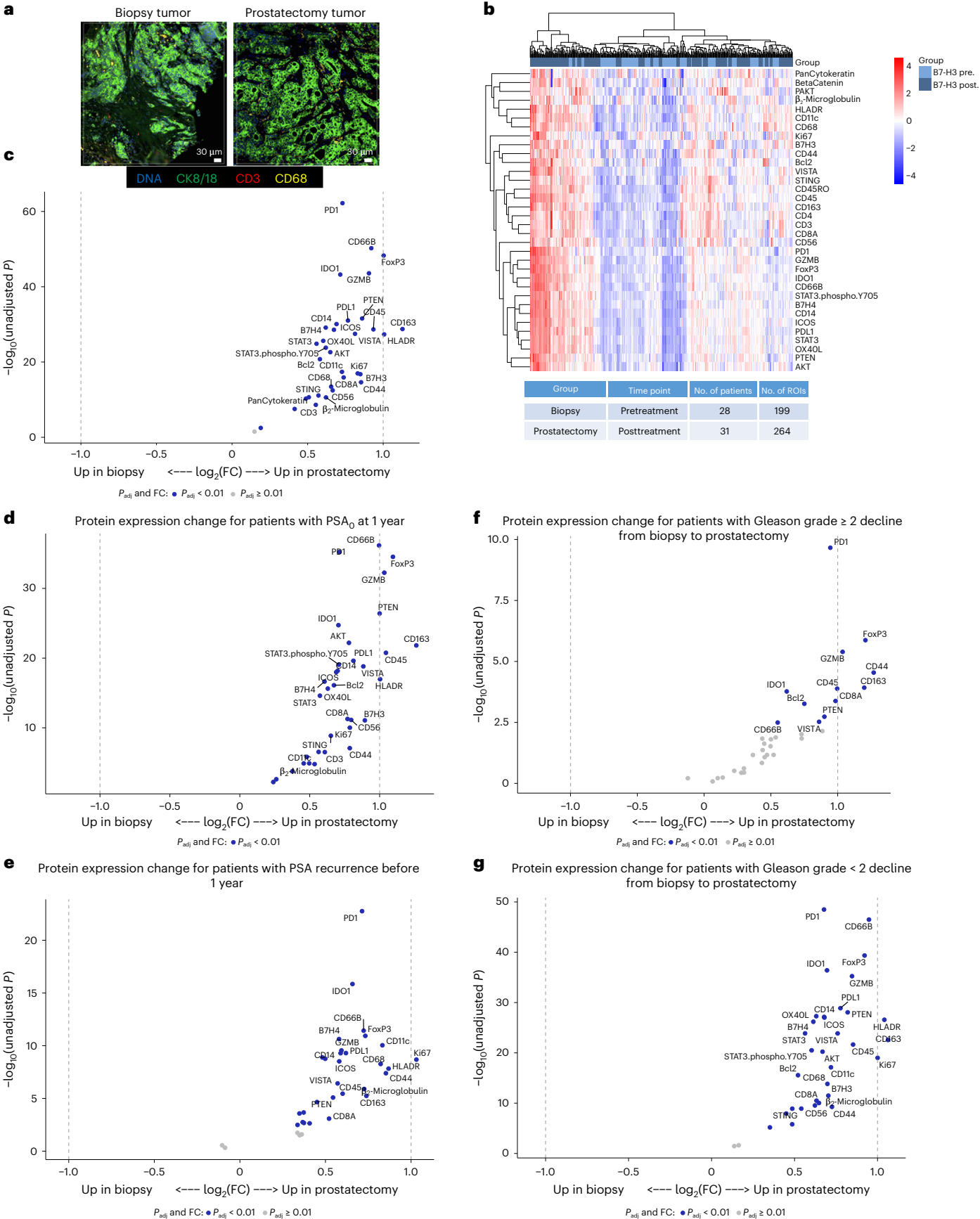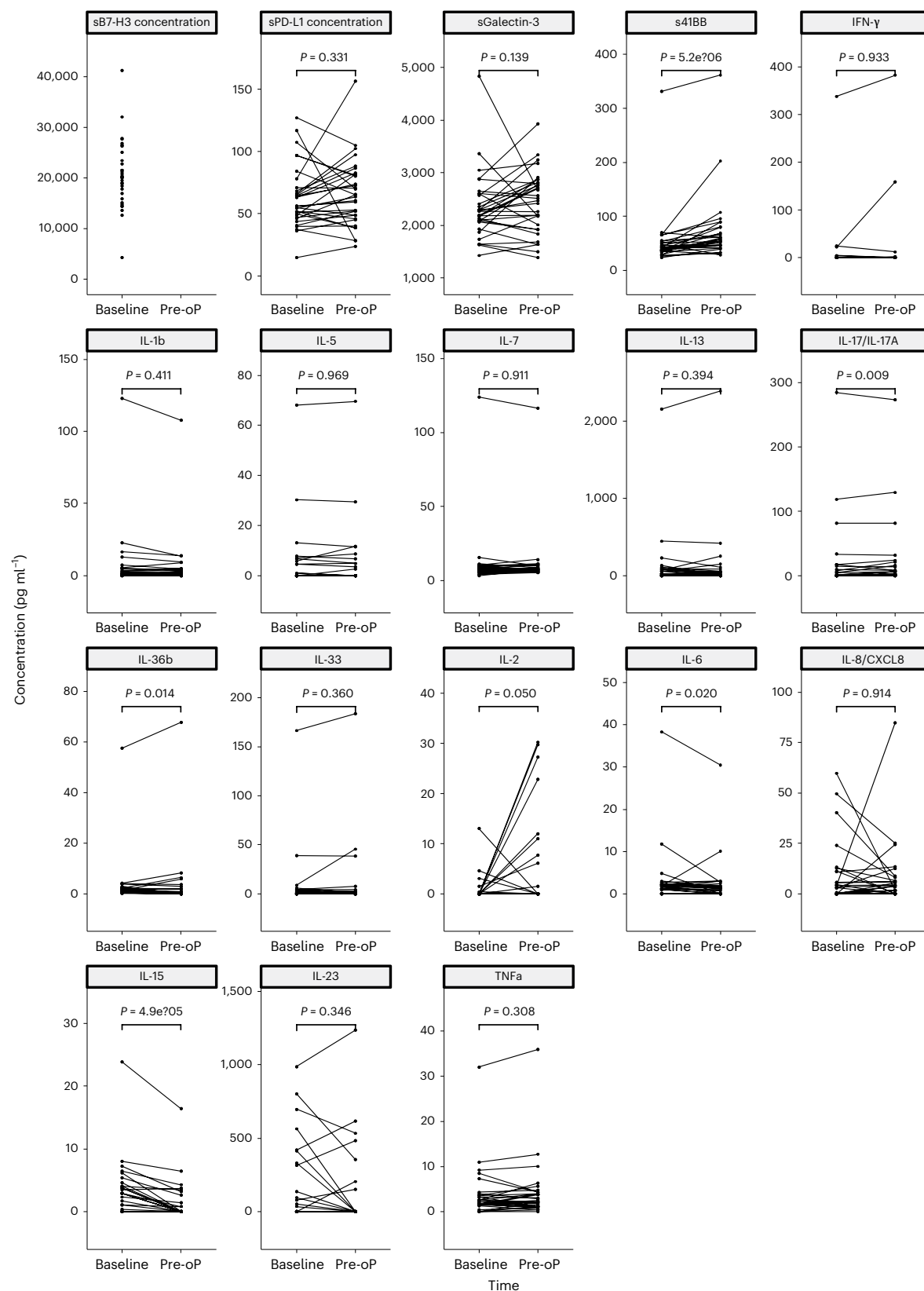
Fig. 4 | Changes in circulating cytokines, chemokines and soluble protein levels from baseline to preprostatectomy (D50). Cytokine analysis was performed from n = 32 patients using n = 64 samples. Only baseline soluble B7-H3 (sB7-H3) levels are shown due to posttreatment ELISA interference from enoblituzumab. Pre-op, preoperative. Two-sided, paired-sample, Wilcoxon's signed-rank test was used to compare cytokine levels between two time points. No adjustment was performed for multiple testing.

of IFN-γ-driven immunosuppressive molecules, such as PD-L1 and influx of FoxP3-positive cells, setting up the possibility of combining B7-H3 ADCC-driven therapy with anti-PD-L1/PD-1 dual therapy.

Exploration of the association between enoblituzumab treatment and the wider systemic immune response showed no prognostic baseline association between any of the tested biomarkers. Increased circulating levels of IL-6 and IL-15 have been associated with PCa and poor outcomes, so decreased levels posttreatment, as observed herein, may be consistent with decreased tumor activity[28,29]. IL-2 (anti-tumoral and T cell and natural killer (NK) cell growth factor) and IL-36β (anti-tumoral IL-2 inducer promoting T cell survival and polarization of helper type 1 T cells (T_H1 cells)) were both elevated posttreatment, consistent with TME T_H1 cell effector response[30,31]. IL-17 was noted to increase posttreatment and all patients with a PSA_0 response at 1 year whose peripheral expanded clones 100% matched their intratumorally expanded clones exhibited IL-17 increase. Further work will be required to elucidate the significance of this finding, because the role of IL-17 in tumorigenesis is still being explored with both pro- and anti-tumor immunity roles described. Finally, soluble 4-1BB (CD137) was increased posttreatment and again specifically in all patients with a PSA_0 response at 1 year whose peripheral expanded clones were 100% matched to their intratumorally expanded clones. The 4-1BB on CD8 T cells has been shown to be costimulatory with proliferative, anti-apoptotic, exhaustion-reversing and pro-effector function-promoting effects[32]. Soluble 4-1BB increase has recently been described as a biomarker of 4-1BB stimulation[33].

It is notable that we did not see off-target autoantibody or antigen spread, except for complement C1r (*C1R*) and basic salivary proline-rich protein 1 (PRB1)-directed antibody signals of unclear significance, from the observed TME inflammatory changes, possibly accounting for the limited toxicity observed. Together, these results define a favorable TME (including increased CD8, GZMB and IL-18 signals), suggesting new intervention strategies that include B7-H3-targeted approaches in PCa, as well as potential biomarkers of response to B7-H3-directed therapeutics.

Limitations of the present study include the single-arm design, relatively small number of patients, single institution design and short duration of enoblituzumab treatment (6 weeks). No reliable literature control data were available to set the benchmark to compare non-ADT neoadjuvant immunotherapy as per the protocol. Consequently, the primary endpoint of PSA_0 at 1 year was designed with a focus on estimating the effect size for future trial designs. Being a quaternary referral center, many of our nontrial PCa patients are seen for a prostatectomy without further follow-up care within our institution, and hence no reliable control patient data were available for comparative PSA_0 at 1-year analysis that would account for adjuvant or salvage ADT or radiation therapy postprostatectomy. Until a planned, larger randomized trial is completed, the long-term PSA response interpretation is of unknown clinical value. Furthermore, the trial was not powered for the secondary endpoint of Gleason decline and the results need to be viewed as exploratory only, with a possibility of sampling bias accounting for the findings between biopsy and radical prostatectomy. The gene expression and NanoString DSP studies were limited by population level detail not allowing us to identify the specific cell populations responsible for upregulation of immune-suppressive or immune-stimulatory markers such as GZMB. In addition, the DSP data showed a clear batch effect pre-batch correction, due to pretreatment samples being processed in one batch and posttreatment samples in another, which probably reduced the accuracy of the batch correction to some degree. Furthermore, the TCR sequences identified by Vβ-sequencing used in the present study may not have represented the functional T cells or the tumor-specific antigens driving the responses. Cytokine analyses lacked power given the trial's small sample size. Overall, these findings are exploratory and need to be confirmed in larger cohorts.

Despite these limitations, the present study of a PCa application of B7-H3-targeted immunotherapy demonstrated an acceptable safety profile with possibly enhanced clinical outcomes in the setting of a systemic and TME profile indicative of an anti-tumor immune response. These results in patients with high-risk PCa and early recurrence rates, and the broader need for immunotherapeutic strategies with efficacy in PCa, warrant further validation and investigation in larger prospective randomized studies—with a large, adequately powered, randomized neoadjuvant study planned to confirm the findings described in the present study. These findings provide the justification for developing multipronged approaches that include targeting B7-H3 to optimize anti-tumor activity in PCa and other solid malignancies.

Online content

Any methods, additional references, Nature Portfolio reporting summaries, source data, extended data, supplementary information, acknowledgements, peer review information; details of author contributions and competing interests; and statements of data and code availability are available at https://doi.org/10.1038/s41591-023-02284-w.

References

1. Siegel, R. L., Miller, K. D., Fuchs, H. E. & Jemal, A. Cancer statistics, 2022. *CA: A Cancer J. Clinicians* **72**, 7–33 (2022).
2. Shilkrut, M., McLaughlin, P. W., Merrick, G. S., Vainshtein, J. M. & Hamstra, D. A. Treatment outcomes in very high-risk prostate cancer treated by dose-escalated and combined-modality radiation therapy. *Am. J. Clin. Oncol.* **39**, 181–188 (2016).
3. Sundi, D. et al. Outcomes of very high-risk prostate cancer after radical prostatectomy: validation study from 3 centers. *Cancer* **125**, 391–397 (2019).
4. Antonarakis, E. S. et al. The natural history of metastatic progression in men with prostate-specific antigen recurrence after radical prostatectomy: long-term follow-up. *BJU Int.* **109**, 32–39 (2012).
5. Le, D. T. et al. Mismatch repair deficiency predicts response of solid tumors to PD-1 blockade. *Science* **357**, 409–413 (2017).
6. Hodi, F. S. et al. Improved survival with ipilimumab in patients with metastatic melanoma. *N. Engl. J. Med.* **363**, 711–723 (2010).
7. Kantoff, P. W. et al. Sipuleucel-T immunotherapy for castration-resistant prostate cancer. *N. Engl. J. Med.* **363**, 411–422 (2010).
8. Kwon, E. D. et al. Ipilimumab versus placebo after radiotherapy in patients with metastatic castration-resistant prostate cancer that had progressed after docetaxel chemotherapy (CA184-043): a multicentre, randomised, double-blind, phase 3 trial. *Lancet Oncol.* **15**, 700–712 (2014).
9. Shenderov, E. et al. Nivolumab plus ipilimumab, with or without enzalutamide, in AR-V7-expressing metastatic castration-resistant prostate cancer: a phase-2 nonrandomized clinical trial. *Prostate* **81**, 326–338 (2021).
10. Sharma, P. et al. Nivolumab plus ipilimumab for metastatic castration-resistant prostate cancer: preliminary analysis of patients in the checkMate 650 trial. *Cancer Cell* **38**, 489–499. e483 (2020).
11. Chapoval, A. I. et al. B7-H3: a costimulatory molecule for T cell activation and IFN-gamma production. *Nat. Immunol.* **2**, 269–274 (2001).
12. Benzon, B. et al. Correlation of B7-H3 with androgen receptor, immune pathways and poor outcome in prostate cancer: an expression-based analysis. *Prostate Cancer Prostatic Dis.* **20**, 28–35 (2017).
13. Loo, D. et al. Development of an Fc-enhanced anti-B7-H3 monoclonal antibody with potent antitumor activity. *Clin. Cancer Res.* **18**, 3834–3845 (2012).

14. Musolino, A. et al. Immunoglobulin G fragment C receptor polymorphisms and clinical efficacy of trastuzumab-based therapy in patients with HER-2/neu-positive metastatic breast cancer. *J. Clin. Oncol.* **26**, 1789–1796 (2008).

15. Obradovic, A. Z. et al. T-cell infiltration and adaptive treg resistance in response to androgen deprivation with or without vaccination in localized prostate cancer. *Clin. Cancer Res.* **26**, 3182–3192 (2020).

16. Fong, L. et al. Activated lymphocyte recruitment into the tumor microenvironment following preoperative sipuleucel-T for localized prostate cancer. *J. Natl Cancer Inst.* **106**, dju268 (2014).

17. Clynes, R. A., Towers, T. L., Presta, L. G. & Ravetch, J. V. Inhibitory Fc receptors modulate in vivo cytoxicity against tumor targets. *Nat. Med.* **6**, 443–446 (2000).

18. Tobinai, K., Klein, C., Oya, N. & Fingerle-Rowson, G. A review of obinutuzumab (GA101), a novel type II anti-CD20 monoclonal antibody, for the treatment of patients with B-cell malignancies. *Adv. Ther.* **34**, 324–356 (2017).

19. Lee, Y. H. et al. Inhibition of the B7-H3 immune checkpoint limits tumor growth by enhancing cytotoxic lymphocyte function. *Cell Res.* **27**, 1034–1045 (2017).

20. Yonesaka, K. et al. B7-H3 negatively modulates CTL-mediated cancer immunity. *Clin. Cancer Res.* **24**, 2653–2664 (2018).

21. Mendes, A. A. et al. Association of B7-H3 expression with racial ancestry, immune cell density, and androgen receptor activation in prostate cancer. *Cancer* **128**, 2269–2280 (2022).

22. Hogan, S. A. et al. Peripheral blood TCR repertoire profiling may facilitate patient stratification for immunotherapy against melanoma. *Cancer Immunol. Res.* **7**, 77–85 (2019).

23. Han, J. et al. TCR repertoire diversity of peripheral PD-1+CD8+ T cells predicts clinical outcomes after immunotherapy in patients with non–small cell lung cancer. *Cancer Immunol. Res.* **8**, 146–154 (2020).

24. Thorsson, V. et al. The immune landscape of cancer. *Immunity* **48**, 812–830.e814 (2018).

25. Haffner, M. C. et al. Comprehensive evaluation of programmed death-ligand 1 expression in primary and metastatic prostate cancer. *Am. J. Pathol.* **188**, 1478–1485 (2018).

26. Antonarakis, E. S. et al. Pembrolizumab for treatment-refractory metastatic castration-resistant prostate cancer: multicohort, open-label phase II KEYNOTE-199 study. *J. Clin. Oncol.* **38**, 395–405 (2019).

27. Graff, J. N. et al. A phase II single-arm study of pembrolizumab with enzalutamide in men with metastatic castration-resistant prostate cancer progressing on enzalutamide alone. *J. Immunother. Cancer* **8**, e000642 (2020).

28. Mengus, C. et al. Elevated levels of circulating IL-7 and IL-15 in patients with early stage prostate cancer. *J. Transl. Med.* **9**, 162 (2011).

29. Dorff, T. B. et al. Clinical and correlative results of SWOG S0354: a phase II trial of CNTO328 (siltuximab), a monoclonal antibody against interleukin-6, in chemotherapy-pretreated patients with castration-resistant prostate cancer. *Clin. Cancer Res.* **16**, 3028–3034 (2010).

30. Waldmann, T. A. Cytokines in cancer immunotherapy. *Cold Spring Harb. Perspect. Biol.* **10**, a028472 (2018).

31. Vigne, S. et al. IL-36 signaling amplifies Th1 responses by enhancing proliferation and Th1 polarization of naive CD4+ T cells. *Blood* **120**, 3478–3487 (2012).

32. Williams, J. B. et al. The EGR2 targets LAG-3 and 4-1BB describe and regulate dysfunctional antigen-specific CD8+ T cells in the tumor microenvironment. *J. Exp. Med.* **214**, 381–400 (2017).

33. Glez-Vaz, J. et al. Soluble CD137 as a dynamic biomarker to monitor agonist CD137 immunotherapies. *J. Immunother. Cancer* **10**, e003532 (2022).

Methods

Study design and patient eligibility

This was a single-institution, open-label, phase 2 study conducted at the Johns Hopkins Hospital. The study had a single arm and there was no randomization. Eligible men with histologically confirmed and operable, intermediate and high-risk localized PCa (Gleason-grade groups 3–5) were enrolled to evaluate the safety, anti-tumor efficacy and immunogenicity of enoblituzumab when given before prostatectomy. Patients were staged with computed tomography (CT) of the chest/abdomen/pelvis and nuclear medicine bone scans before enrollment. Key inclusion criteria included: histological adenocarcinoma; clinical stage T1c–T3b, N0, M0; Gleason score $4 + 3 = 7$ to $5 + 5 = 10$ (grade group 3–5); at least 2 positive biopsy cores; prior decision to undergo radical prostatectomy; adult male aged >18 years; and ECOG performance status 0–1. Key exclusion criteria included: previous hormones, biologics or chemotherapy for PCa; previous immunotherapy/vaccine therapy for PCa; and history of autoimmune disease requiring systemic immunosuppression. Detailed eligibility criteria are presented in the study protocol. All patients who met the eligibility criteria (denominator unknown) were approached about the study by their treating Johns Hopkins urologist. Those who expressed potential interest ($n = 75$) were provided the informed consent and were referred to the research nurse for additional discussion. After signing consent, patients received enoblituzumab (15 mg kg^{-1} intravenously weekly, for a total of six doses) starting 50 days before radical prostatectomy. Then, 14 days after the last dose of study drug, patients underwent prostatectomy and the prostate glands were harvested and examined for pathological and immunological endpoints. The prostatectomy specimen tumor block with the highest-grade tumor located in the prostate was selected and microtome paraffin-embedded sections were prepared for biological analysis. Study assessments were prospectively defined. Safety was assessed by collecting and grading AEs according to Common Terminology Criteria for Adverse Events (CTCAE) v.4.0 criteria. Each patient was counted only once at the highest grade of any AE for that patient. Follow-up evaluation for AEs occurred 30 days and 90 days after surgery. Patients were then followed by their urologists according to standard institutional practices, with PSA evaluations every 3 (±1) months during year 1 and every 6 (±2) months during years 2–3. Half-way through the study, the study was amended and expanded to enroll an additional 16 patients, making a total of 32 patients, to continue evaluating safety and adjust the sample size for a better descriptive estimation of the clinical benefit of enoblituzumab in terms of undetectable PSA level (<0.1 ng ml−1) at 12 months after radical prostatectomy. Clinical data were collected in a protected institutional clinical research management system.

This was an investigator-initiated trial (NCT02923180) funded by MacroGenics, Inc., which also provided the study drug free of cost. The study and study amendment were approved by the Johns Hopkins University institutional review board and overseen by an independent scientific review committee and a data and safety monitoring committee. The study was performed in accordance with the Declaration of Helsinki and Good Clinical Practice guidelines. All patients provided written informed consent before participation.

Endpoints and clinical study assessments

The coprimary outcomes were safety and feasibility of enoblituzumab administration in the neoadjuvant setting and PSA_0 response (PSA level <0.1 ng ml^{-1}) at 12 months after radical prostatectomy. The statistical design for the coprimary endpoint of PSA_0 at 12 months was descriptive, with the goal being to estimate the PSA_0 rate at 12 months with 95% CI, rather than hypothesis testing. Consequently, neither of the coprimary endpoints had a power calculation included. Secondary clinical endpoints included Gleason-grade group change from biopsy to posttreatment prostatectomy, number of participants who achieve pathological complete response, defined as absence of tumor

identification on standard histological analysis of resected prostate specimens, and time to PSA recurrence, defined as time from prostatectomy to time when PSA was ≥0.2 ng ml^{-1} (estimated using the Kaplan–Meier method) or progression. Trial progression was defined as time from prostatectomy to time when PSA was ≥0.2 ng ml^{-1} (confirmed by a second PSA of the same level or higher) or start of salvage or adjuvant ADT or radiation therapy when clinically indicated, whichever occurred first. Secondary biomarker endpoints included enoblituzumab drug distribution in tumor tissue on fresh frozen sections, density of CD8$^+$ T cells in harvested prostate glands from treated patients, mean staining percentage of PD-L1 in tumor tissue in primary core biopsies (pretreatment) and prostatectomy surgical specimens (posttreatment), quantification of markers of apoptosis, quantification of proliferation using Ki-67, regulatory T cell density, CD4$^+$ T cell density and NK cell density in prostatectomy (posttreatment). Toxicity was monitored continuously with early stopping rules for AEs and/or surgical complications.

PSA measurements were obtained at baseline and at radical prostatectomy (day 50)−6 weeks apart, as well as during follow-up as per study design. Radiographic evaluations (CT of chest/abdomen/pelvis and technetium-99 bone scans) were performed at baseline. Physical examination, toxicity assessments and laboratory studies (complete blood count and comprehensive metabolic panel) were performed every week on treatment and during follow-up on days 30 and 90 postradical prostatectomy.

Enoblituzumab tissue distribution

Enoblituzumab prostate tissue penetrance was evaluated using immunohistochemical staining of frozen posttreatment prostatectomy tissue utilizing rabbit anti-enoblituzumab antibody (MacroGenics proprietary monoclonal antibody) and compared with anti-B7-H3 staining utilizing rabbit anti-human B7-H3 monoclonal antibody clone SP206 (Spring Biosciences, catalog no. M5064.C). Primary antibody staining of enoblituzumab (0.1–0.5 µg ml^{-1}, 15 min) and SP206 (0.2 µg ml^{-1}, 30 min) was performed on adjacent 7-µm-thick frozen sections pretreated with peroxidase blocking reagent and 5% normal goat serum, followed by Agilent Envision anti-rabbit polymer for 20 min at room temperature and incubation with 3,3′-diaminobenzidine for 3 min to visualize reactivity. H-score (range 0–300) was calculated as the combined sum of staining intensities (0, 1+, 2, 3+) multiplied by the percentage of positive cells (membranous and/or cytoplasmic) for each intensity.

Whole-exome DNA and whole-transcriptome RNA-seq analysis

Tumor and matched normal (blood) specimens from 32 patients underwent commercial CAP/CLIA-grade next-generation sequencing testing with the Tempus xE assay, a hybrid-capture, whole-exome panel combined with whole-transcriptome RNA-seq. The assay detects single nucleotide variants, insertions and deletions (indels), and copy number variants, as well as gene fusions (translocations) and loci for MSI assessment. FFPE tumor specimen content was enriched to at least 40% post-macrodissection and sequenced on an Illumina NovaSeq 6000. Analyses were performed on tumor samples with matched normal peripheral blood mononuclear cell DNA subtraction. Only protein-truncating alterations, known pathogenic missense changes or ClinVar[34]-designated pathogenic alterations were classified as deleterious in the current analysis.

TCR-seq and assessment of the TCR repertoire

Genomic DNA from baseline peripheral blood lymphocytes, posttreatment D50, peripheral blood lymphocytes and posttreatment D50, radical prostatectomy, fresh frozen tumor tissue was extracted with QIAsymphony using the tissue extraction method (QIAGEN), and immunosequencing of the CDR3 regions of human TCR-β chains was performed using the ImmunoSEQ Assay (Adaptive Biotechnologies).

Sequences were collapsed and filtered to identify and quantify the absolute abundance of each unique TCR-β CDR3 region for further analysis[35,36]. To estimate the fraction of T cells in the samples, 6.5 pg of DNA was estimated per diploid cell and normalized the total T cell counts in each sample to the amount of input DNA.

To assess peripheral clonal dynamics and compare individual clones across samples from the same subject, the number of expanded clones in each posttreatment sample, compared with baseline sample, was calculated according to a binomial distribution framework[37]. In brief, a two-sided test of the null hypothesis that the probability of success in a Bernoulli experiment is P is computed for each clone. A Benjamini–Hochberg multiple testing correction was applied and clones were selected at $\alpha = 0.1$. To identify expanded clones that were present in the tumor sample, an exact match on the CDR3 amino acid sequence between an expanded clone and a clone in the tumor sample was required.

Serum cytokine, chemokine and soluble protein profiling

Patient baseline and D50 sera were collected in 10 ml of tiger-top vacutainer tubes (BD Biosciences) and processed within 6 h of collection. Processing involved 20 min for coagulation and centrifugation at 25 °C for 15 min at 1,500g. Customized Luminex ELISA was performed in duplicates as per the manufacturer's instructions (R&D Systems, a Bio-Techne brand). The analytes included in these studies were soluble B7-H3, soluble PD-L1, soluble galectin-3, soluble 4-1BB, IFN-γ, IL-2, Il-1b, IL-5, IL-7, IL-13, IL-17, IL-36b, IL-33, IL-6, IL-8, IL-15, IL-23 and tumor necrosis factor (TNF)-α. Wilcoxon's signed-rank test was used to compare cytokine levels between two time points. Associations with clinical outcomes were analyzed using the lower tertile group (≤33rd percentile) compared against the middle and upper tertile groups (>33rd percentile).

RNA expression profiling of the TME

Gene expression profiling was performed on FFPE prostate tissue from all 32 patients and 32 matched one-to-one untreated control patients. Extracted RNA was analyzed utilizing the nCounter PanCancer IO 360 panel (NanoString Technologies). All samples were prepared and run as a single batch with a PanCancer IO 360 panel standard per cartridge to minimize the batch effect.

Gene counts were normalized using a ratio of the expression value to the geometric mean of 20 housekeeping genes in the Pan-Cancer IO 360 panel[15]. Housekeeping-normalized genes were then normalized using a ratio of the panel standard run on each cartridge. Housekeeper-normalized and panel standard-normalized data are then log$_2$(transformed). For each pairwise comparison, Benjamini and Yekutieli's false discovery rate (FDR) correction was performed and the number of differentially upregulated and downregulated genes with a corrected $P < 0.05$ or $P < 0.01$ was reported.

Digital spatial proteomic profiling of the TME

Whole-slide FFPE tissue cores from biopsy (pretreatment) and prostatectomy (posttreatment) whole-slide tissue sections were profiled utilizing GeoMx DSP (NanoString Technologies)[38]. Tissue morphology was visualized using fluorescent cytokeratin (CK)8/18 Alexa Fluor-532 (clone K8.8+DC10, Novus, catalog no. NBP2-34655AF532, 2.3 μg ml^{-1}), CD3 Alexa Fluor-594 (clone UMAB54, Origene, 3.6 μg ml^{-1}) and CD68 Alexa Fluor-647 (clone KP1, Santa Cruz, catalog no. sc-20060 AF647, 1.4 μg ml^{-1}) antibodies, as well as Cyto83 to detect nucleic acids. ROIs of ~600-μm geometric shapes (squares and circles) were selected in either tumor or benign areas. DSP Human Protein Immune Cell Profiling and IO Panels were assessed using an nCounter-based readout.

Digital spatial proteomic profiling data were processed from images to counts following the manufacturer's instructions. Low-quality samples were removed from analysis if: <250 fields of view were successfully counted and imaged; binding density was <0.1

or >2.25 optical features per μm^2; the geometric mean of counts from positive control probes A:D, targeting spike-in controls, was <1,000; or the counts from positive control probe E, also targeting a spike-in control, were less than the mean of the negative control probes + 2 s.d.s. Data were then normalized to the geometric mean of positive control probes A:D to account for nCounter-associated technical variation. Samples with low S6 and H3 histone housekeeper expression were then removed, and data were normalized to the geometric mean of the housekeepers to account for digital spatial profiler (DSP)-associated technical variation and some biological variations, such as cellularity. A clear batch effect was observed in the data. For correction, log$_2$(expression data) was fit with a linear model, 'protein_target ~ 1+ (1|Batch)', using lmerTest 3.1-3 in R v.4.2.0. Residuals and the intercept of the fixed effect were each exponentiated back to the linear scale. Residuals were then multiplied by the intercept to become batch-corrected expression data. Sample conditions were not evenly distributed across batches, which reduces the accuracy of this batch correction method. Notably, all pretreatment samples were in batch 1, whereas posttreatment samples spanned batches 1 and 2. Differential expression was tested with a linear model, 'protein_target ~ Timepoint+ (1 | Patient)', using lmerTest 3.1-3; the patient was used as a random effect (with random intercept) with the degrees of freedom estimated using Satterthwaite's method. Raw P values were adjusted based on an FDR level of 0.01 using the Benjamini–Hochberg procedure to account for multiple hypothesis testing.

Serum autoantibody profiling

Serum autoantibodies from all 32 patients were profiled utilizing a human proteome microarray (HuProt Human Proteome Microarray v.4.0, CDI Laboratories) that contains >21,000 unique, individually purified, full-length human proteins in duplicate, covering >81% of the proteome[39]. Briefly, the HuProt arrays were blocked with blocking solution (5% bovine serum albumin/1× Tris-buffered saline + Tween 20 (TBS-T)) at room temperature for 1 h, and then probed with the serum samples (diluted 1:1,000) at 4 °C overnight. The arrays were then washed 3× with 1× TBS-T, 10 min each, and probed with 0.25 μg ml^{-1} of Alexa Fluor-647-labeled anti-human IgG Fcγ fragment specific (polyclonal, Jackson ImmunoResearch, catalog no. 109-606-098) and 0.25 μg ml^{-1} of Cy3-labeled anti-human IgM Fc5μ fragment-specific secondary antibodies (polyclonal, Jackson ImmunoResearch, catalog no. 109-165-043) at room temperature for 1 h, followed by three washes of 1× TBS-T, 10 min each, and then dried with an air duster and scanned using a GenePix 4000B instrument (Molecular Devices). GenePix Pro (v.7.2.30) software was used to measure the signal intensities for IgG and IgM binding to array features.

Statistical analyses

Baseline patient demographics and clinical characteristics as well as pathology outcomes posttreatment were summarized with count and percentage for categorical variables and mean (s.d.) and median (range) for continuous variables. For biomarker analysis, patients missing particular biomarker data were excluded for that specific biomarker comparison. Waterfall plots were used to display percentage change in PSA from screening to pre-prostatectomy and Gleason-grade group change from biopsy to prostatectomy. The time-to-event endpoint of time to PSA recurrence (PSA ≥ 0.2 ng ml^{-1}) was analyzed using the Kaplan–Meier method. For exploratory biomarkers, P_{adj} values were computed using the Benjamini–Hochberg correction. Kaplan–Meier curves for PSA recurrence-free survival were compared by mutational groups using the log(rank test) with Cox's proportional-hazard models to estimate hazard ratios. Fisher's exact test was used to assess association between mutation groups and the primary binary outcome. Changes in cytokine levels between two time points, baseline and pre-prostatectomy, were examined using Wilcoxon's signed-rank test. Univariate and multivariate logistic regression with adjustment for

age were used to summarize odds ratios of biomarkers for each binary clinical outcome, comparing their odds between lower tertile versus middle and upper tertiles of baseline cytokine levels. All tests were two sided and $P \leq 0.05$ was considered statistically significant. Statistical analyses were performed using R (v.4.2.2) and GraphPad Prism v.9.3.1.

Reporting summary

Further information on research design is available in the Nature Portfolio Reporting Summary linked to this article.

Data availability

TRV-β-seq of tumor and peripheral T cells, as the project 'Neoadjuvant B7H3 Trial in Prostate Cancer', is available in the immuneACCESS free public database at https://clients.adaptivebiotech.com/immuneaccess. The authors deferred trial participant raw genomic data deposition to national or international public repositories to avoid compromising privacy of the research participants. A summary of patient whole-exome sequence alterations of clinical significance is provided in Supplementary Data Table 4. Aggregate patient-related information has been made available on ClinicalTrials.gov (https://clinicaltrials.gov/ct2/show/results/NCT02923180). Additional requests for raw and analyzed data can be referred to the corresponding author (E.S.) and will be reviewed promptly as part of a data transfer agreement per Johns Hopkins' institutional policies, to determine whether the request is subject to any clinical trial patient confidentiality or intellectual property requirements. Source data are provided with this paper.

References

34. Landrum, M. J. et al. ClinVar: public archive of interpretations of clinically relevant variants. *Nucleic Acids Res.* **44**, D862–D868 (2016).
35. Robins, H. S. et al. Comprehensive assessment of T-cell receptor beta-chain diversity in alphabeta T cells. *Blood* **114**, 4099–4107 (2009).
36. Carlson, C. S. et al. Using synthetic templates to design an unbiased multiplex PCR assay. *Nat. Commun.* **4**, 2680 (2013).
37. DeWitt, W. S. et al. Dynamics of the cytotoxic T cell response to a model of acute viral infection. *J. Virol.* **89**, 4517–4526 (2015).
38. Merritt, C. R. et al. Multiplex digital spatial profiling of proteins and RNA in fixed tissue. *Nat. Biotechnol.* **38**, 586–599 (2020).
39. Jeong, J. S. et al. Rapid Identification of monospecific monoclonal antibodies using a human proteome microarray*. *Mol. Cell. Proteom.* **11**, O111.016253 (2012).

Acknowledgements

Author contributions

E.S., E.S.A., D.M.P., C.G.D. and A.E.R. conceived and designed the study. E.S.A., D.P. and C.G.D. supervised the study. E.S., M.E.A., C.C., S.R.D., K.J.P. and C.P.P. recruited and coordinated the participants. E.S., A.M.D.M., T.L.L., C.C., P.M., H.W., S.C., S.J.L., H.J., F.C., K.S., A.M.W., S.E.C., B.H., P.F., S.H. and E.S.A. collected, processed and analyzed the data. E.S. and E.S.A. prepared the manuscript, with all the authors contributing to its review and editing.

Competing interests

Additional information

Extended Data Fig. 1 | Clinical trial flow chart showing biospecimen collection time schema. Created with BioRender.com.
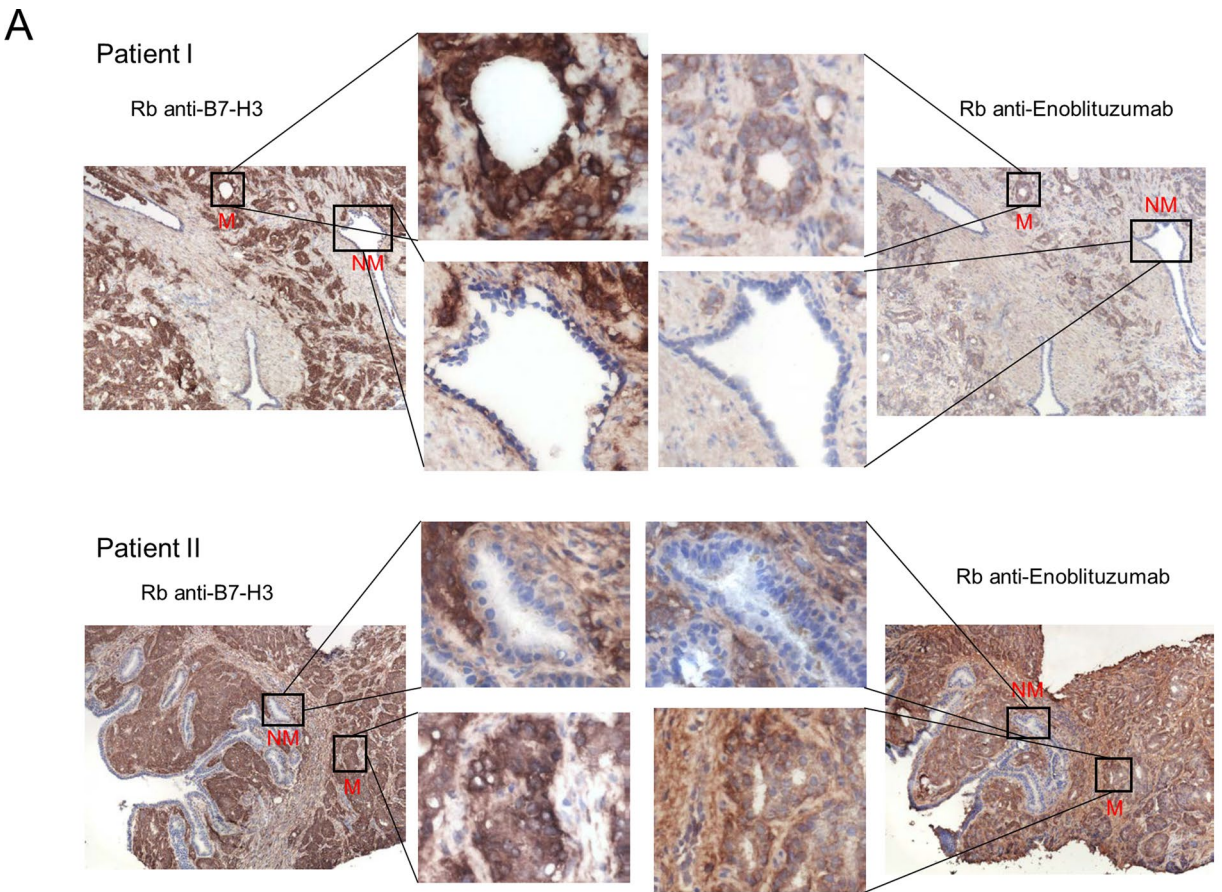
B

	Overall
	(N=32)
Enoblituzumab on tumor (frozen)	
Positive	28 (88%)
Negative	2 (6%)
Not Evaluable	2 (6%)
SP206 anti-B7-H3 on tumor (frozen)	
Evaluable	30 (94%)
Not Evaluable	2 (6%)
H-score, median (range)	242.5 (150-280)

Extended Data Fig. 2 | B7-H3 Expression vs. Enoblituzumab Drug Distribution in post-enoblituzumab treated prostatectomy tissue. a, Two illustrative patients. Small malignant glands (M) showed obvious membrane staining by both SP206 anti-B7-H3 and anti-enoblituzumab antibody IHC staining. However, the adjacent non-malignant ducts (NM) showed relative negative membrane staining for both test articles. **b,** Frequency table of enoblituzumab positive or negative staining on post-enoblituzumab treated prostatectomy frozen sections, as well as SP206 anti-B7-H3 H-score on adjacent treated prostatectomy frozen sections. Image acquired using 20× magnification.

Extended Data Fig. 3 | B7-H3 Expression vs. Enoblituzumab Drug Distribution in post-enoblituzumab treated prostatectomy tissue. Orange bars show enoblituzumab treated patients and gray bars show untreated control 1:1 matched prostatectomies from patients matched by grade group, stage, margins, block age [within 2 years], age [within 2 years], and self-reported race. No bar shown if no change in Gleason between biopsy and prostatectomy.

Extended Data Fig. 4 | TCR repertoire characterization in peripheral blood and tumor by PSA$_0$ at 1-year. (**a**, **b**) Total T-cells expanded in tumor (**a**) or peripheral blood at prostatectomy (**b**, D50) versus fraction of peripheral clones expanded and detected intratumorally. (**c**, **d**) Total unique T-cell clonotypes expanded in tumor (**c**) or peripheral blood at prostatectomy (**d**, D50) versus fraction of peripheral clones expanded and detected intratumorally. Each point on the scatter plots represents a patient. Blue dots indicate responders for a given outcome and red dots indicate non-responders.
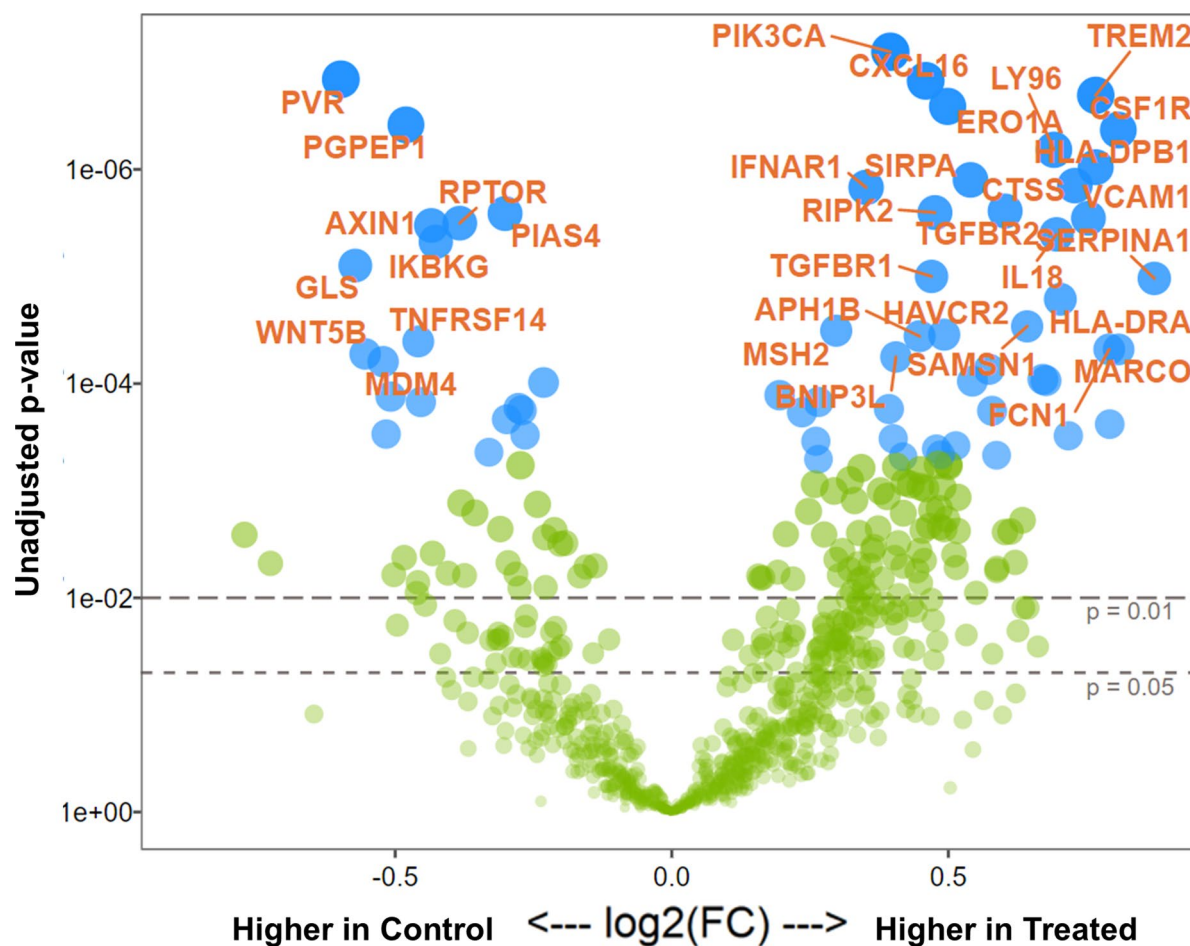
Extended Data Fig. 5 | Volcano plot of tumor region mRNA expression changes of matched untreated control prostatectomies versus post-treatment prostatectomies by Nanostring PanCancer IO 360 analysis. Genes that remained significant after Benjamini and Yekutieli False Discovery Rate (FDR, adjusted *p < 0.01*) are in blue and labeled. Matched 1:1 untreated controls by grade group, stage, margins, block age [within 2 years], age [within 2 years], and self-reported race. Tumor regions isolated by macrodissection.

A Change in protein expression by PSA₀ at 12 months

B Change in protein expression by Gleason grade change
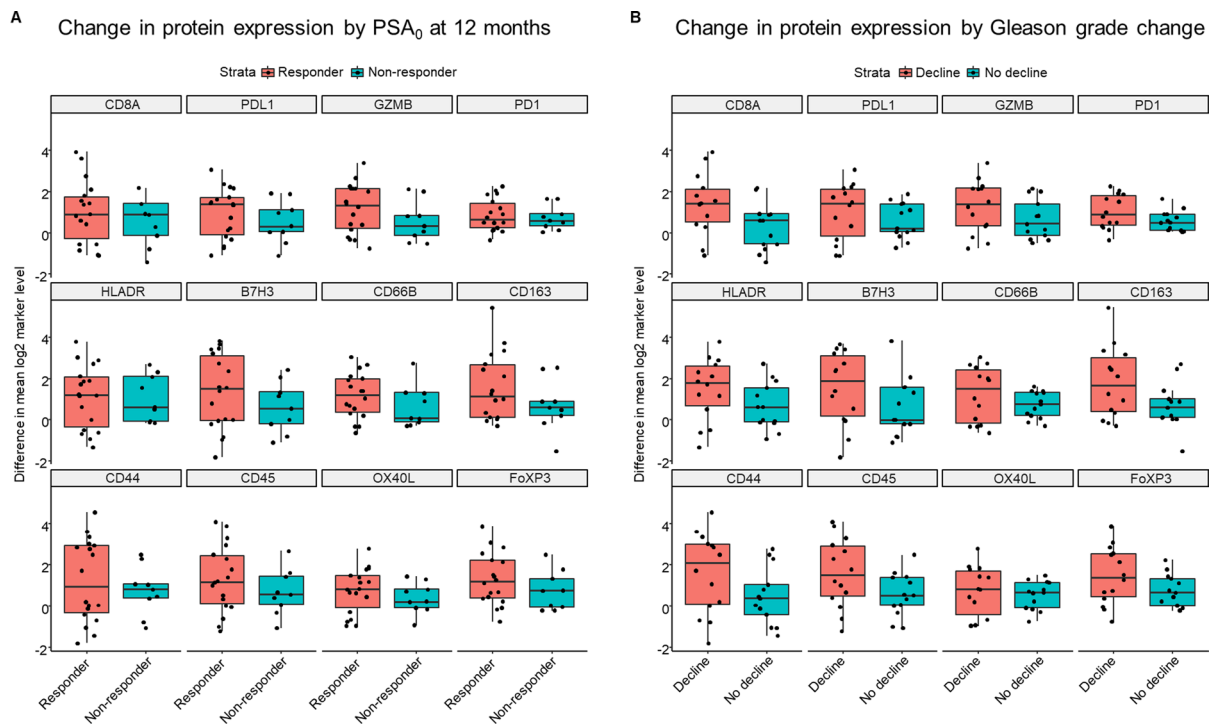
Extended Data Fig. 6 | Grouped boxplots of difference in mean log2 marker level of upregulated proteins by clinical outcome using DSP of the TME in pretreatment biopsies and post-treatment prostatectomies following B7-H3 monoclonal antibody treatment. a, protein marker status by PSA response (PSA < 0.1 ng/mL) at 12 months after prostatectomy versus PSA recurrence. Protein expression was assessed in n = 27 tissue samples from n = 32 patients (n = 18 responders and n = 9 non-responders). **b**, protein marker status by Gleason grade group change from biopsy to prostatectomy. Protein expression was assessed in n = 27 tissue samples from n = 32 patients (n = 14 decline in Gleason and n = 13 no decline in Gleason). Median (IQR) data is presented and whiskers indicate the minimum and maximum values.
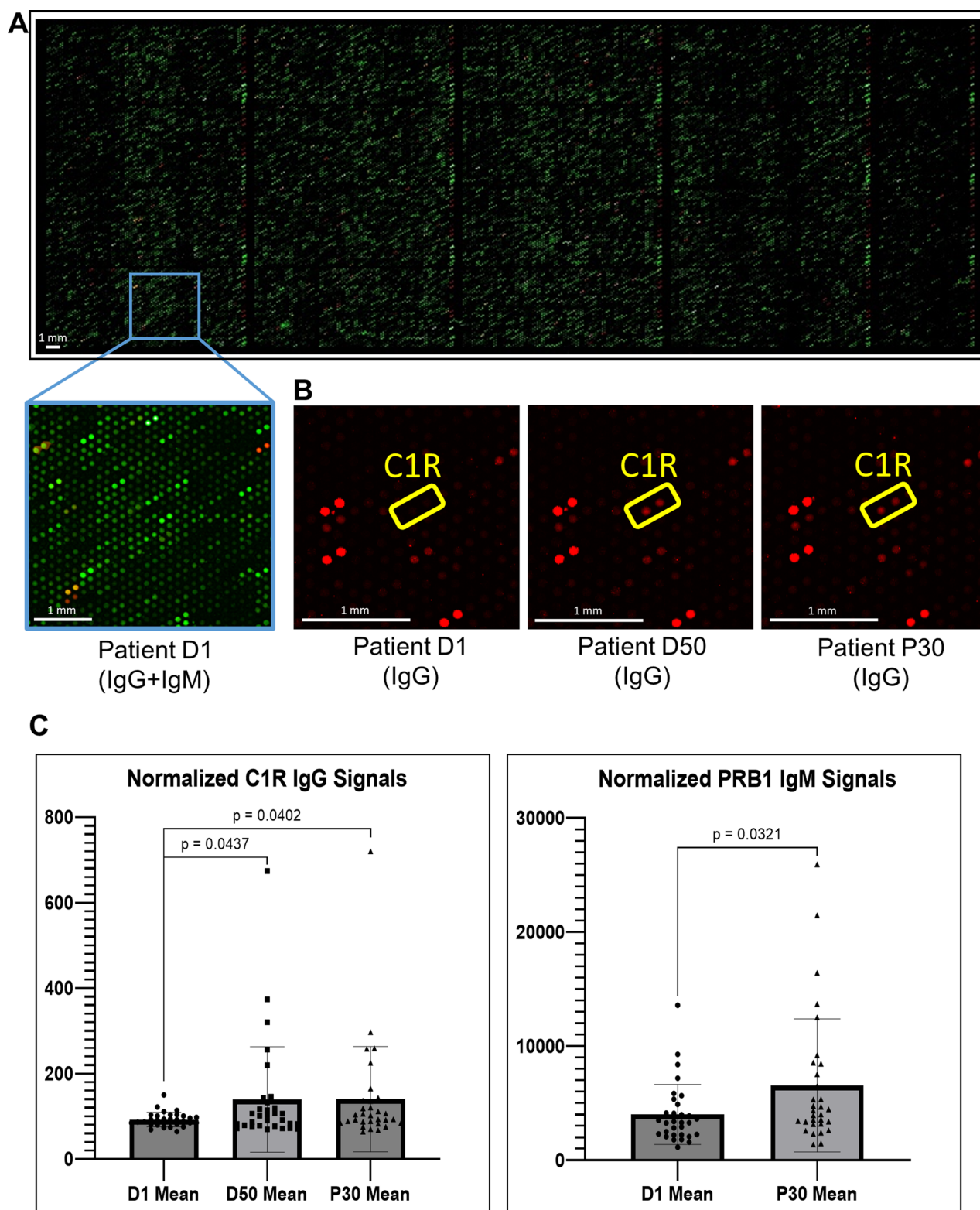
Extended Data Fig. 7 | Treatment-induced antibody reactivity assessment. **a**, A HuProt array probed with a representative patient serum (baseline, D1) and detected with anti-human IgG (red) and anti-human IgM (green) secondary antibodies. Each protein is printed in duplicate diagonally. **b**, Serum samples of the representative patient collected immediately prior to prostatectomy (D50) and 30-days post-prostatectomy (P30) showed significantly higher IgG signals than baseline (D1) on C1R. **c**, The mean C1R IgG signals of all 32 patients at D50 and P30 are significantly higher than D1 (p < 0.05). The mean PRB1 IgM signal of all 32 patients at P30 is significantly higher than D1 (p < 0.05). Two-sided, unpaired, student t-test utilized and standard deviation bars shown.

A

Biomarkers	Decline =>2 <=33rd percentile	Decline =>2 >33rd percentile
sB7-H3 Conc	3 (27.3)	4 (19.0)
sPD-L1 Conc	2 (18.2)	5 (23.8)
sGalectin-3	2 (18.2)	5 (23.8)
s41BB	2 (14.3)	5 (27.8)
IFNg	5 (19.2)	2 (33.3)
IL-1b	1 (9.1)	6 (28.6)
IL-5	5 (23.8)	2 (18.2)
IL-7	3 (27.3)	4 (19.0)
IL-13	3 (27.3)	4 (19.0)
IL-17/IL-17A	5 (26.3)	2 (15.4)
IL-36b	2 (16.7)	5 (25.0)
IL-33	2 (16.7)	5 (25.0)
IL-2	7 (25.9)	0 (0.0)
IL-6	2 (18.2)	5 (23.8)
IL-8/CXCL8	1 (7.1)	6 (33.3)
IL-15	3 (27.3)	4 (19.0)
IL-23	3 (15.8)	4 (30.8)
TNFa	2 (18.2)	5 (23.8)

B — Unadjusted Odds Ratio

Biomarkers	Unadjusted Odds Ratio
sB7-H3 Conc	0.63 (0.11, 3.81)
sPD-L1 Conc	1.41 (0.24, 11.24)
sGalectin-3	1.41 (0.24, 11.24)
s41BB	2.31 (0.41, 18.3)
IFNg	2.1 (0.24, 14.51)
IL-1b	4 (0.56, 81.65)
IL-5	0.71 (0.09, 4.1)
IL-7	0.63 (0.11, 3.81)
IL-13	0.63 (0.11, 3.81)
IL-17/IL-17A	0.51 (0.06, 2.88)
IL-36b	1.67 (0.29, 13.26)
IL-33	1.67 (0.29, 13.26)
IL-2	0 (NA, 4.4e+122)
IL-6	1.41 (0.24, 11.24)
IL-8/CXCL8	6.5 (0.92, 132.41)
IL-15	0.63 (0.11, 3.81)
IL-23	2.37 (0.43, 14.44)
TNFa	1.41 (0.24, 11.24)

C — Adjusted Odds Ratio

Biomarkers	Adjusted Odds Ratio
sB7-H3 Conc	0.66 (0.12, 4.08)
sPD-L1 Conc	1.31 (0.22, 10.63)
sGalectin-3	1.25 (0.2, 10.29)
s41BB	2.16 (0.37, 17.34)
IFNg	1.9 (0.21, 13.56)
IL-1b	3.72 (0.51, 76.79)
IL-5	0.66 (0.08, 3.9)
IL-7	0.64 (0.11, 3.91)
IL-13	0.61 (0.11, 3.77)
IL-17/IL-17A	0.52 (0.07, 3.01)
IL-36b	1.69 (0.29, 13.59)
IL-33	1.43 (0.22, 12.17)
IL-2	0 (NA, 2.2e+108)
IL-6	1.38 (0.23, 11.1)
IL-8/CXCL8	6.33 (0.89, 129.44)
IL-15	0.58 (0.1, 3.62)
IL-23	2.24 (0.4, 13.81)
TNFa	1.39 (0.24, 11.19)

Axis (B and C): 0.05 0.10 0.25 0.50 1.00 2.00 5.00 10.00 20.00 — Lowest tertile does better / Highest 2 tertiles do better

D

Biomarkers	Responder <=33rd percentile	Responder >33rd percentile
sB7-H3 Conc	9 (81.8)	12 (57.1)
sPD-L1 Conc	8 (72.7)	13 (61.9)
sGalectin-3	7 (63.6)	14 (66.7)
s41BB	8 (57.1)	13 (72.2)
IFNg	17 (65.4)	4 (66.7)
IL-1b	7 (63.6)	14 (66.7)
IL-5	16 (76.2)	5 (45.5)
IL-7	9 (81.8)	12 (57.1)
IL-13	7 (63.6)	14 (66.7)
IL-17/IL-17A	12 (63.2)	9 (69.2)
IL-36b	8 (66.7)	13 (65.0)
IL-33	7 (58.3)	14 (70.0)
IL-2	19 (70.4)	2 (40.0)
IL?6	9 (81.8)	12 (57.1)
IL-8/CXCL8	9 (64.3)	12 (66.7)
IL-15	6 (54.5)	15 (71.4)
IL-23	11 (57.9)	10 (76.9)
TNFa	6 (54.5)	15 (71.4)

E — Unadjusted Odds Ratio

Biomarkers	Unadjusted Odds Ratio
sB7-H3 Conc	0.3 (0.04, 1.52)
sPD-L1 Conc	0.61 (0.11, 2.85)
sGalectin-3	1.14 (0.23, 5.25)
s41BB	1.95 (0.45, 8.96)
IFNg	1.06 (0.17, 8.71)
IL-1b	1.14 (0.23, 5.25)
IL-5	0.26 (0.05, 1.2)
IL-7	0.3 (0.04, 1.52)
IL-13	1.14 (0.23, 5.25)
IL-17/IL-17A	1.31 (0.3, 6.32)
IL-36b	0.93 (0.19, 4.17)
IL-33	1.67 (0.37, 7.61)
IL-2	0.28 (0.03, 2)
IL?6	0.3 (0.04, 1.52)
IL-8/CXCL8	1.11 (0.25, 4.89)
IL-15	2.08 (0.45, 9.84)
IL-23	2.42 (0.53, 13.51)
TNFa	2.08 (0.45, 9.84)

F — Adjusted Odds Ratio

Biomarkers	Adjusted Odds Ratio
sB7-H3 Conc	0.28 (0.04, 1.46)
sPD-L1 Conc	0.62 (0.11, 2.97)
sGalectin-3	1.23 (0.24, 5.98)
s41BB	2.08 (0.47, 9.98)
IFNg	1.13 (0.18, 9.58)
IL-1b	1.21 (0.24, 5.83)
IL-5	0.26 (0.05, 1.22)
IL-7	0.29 (0.04, 1.5)
IL-13	1.15 (0.23, 5.3)
IL-17/IL-17A	1.3 (0.29, 6.26)
IL-36b	0.92 (0.19, 4.16)
IL-33	1.95 (0.39, 10.36)
IL-2	0.22 (0.02, 1.76)
IL?6	0.3 (0.04, 1.53)
IL-8/CXCL8	1.14 (0.25, 5.08)
IL-15	2.15 (0.46, 10.39)
IL-23	2.57 (0.55, 14.82)
TNFa	2.1 (0.45, 10)

Axis (E and F): 0.05 0.10 0.25 0.50 1.00 2.00 5.00 10.00 20.00 — Lowest tertile does better / Highest 2 tertiles do better

Extended Data Fig. 8 | Univariate and multivariate analysis of lower tertile versus upper 2 tertiles of serum biomarker alterations by Gleason grade group decline ≥2 or by PSA$_0$ response at 1 year. Serum biomarkers assessed in in n = 64 blood samples from n = 32 patients. **(a-c) By Gleason grade group decline ≥2:** **(a)** Gleason grade group ≥ 2 decline by biomarker and percentile. **(b)** Unadjusted hazard ratio and 95% confidence interval shown for each biomarker. **(c)** Adjusted hazard ratio and 95% confidence interval by age. **(d-f) By PSA0 response at 1 year:** **(d)** PSA$_0$ responders at 1 year by biomarker and percentile. **(e)** Unadjusted hazard ratio and 95% confidence interval shown for each biomarker. **(f)** Adjusted hazard ratio and 95% confidence interval by age.
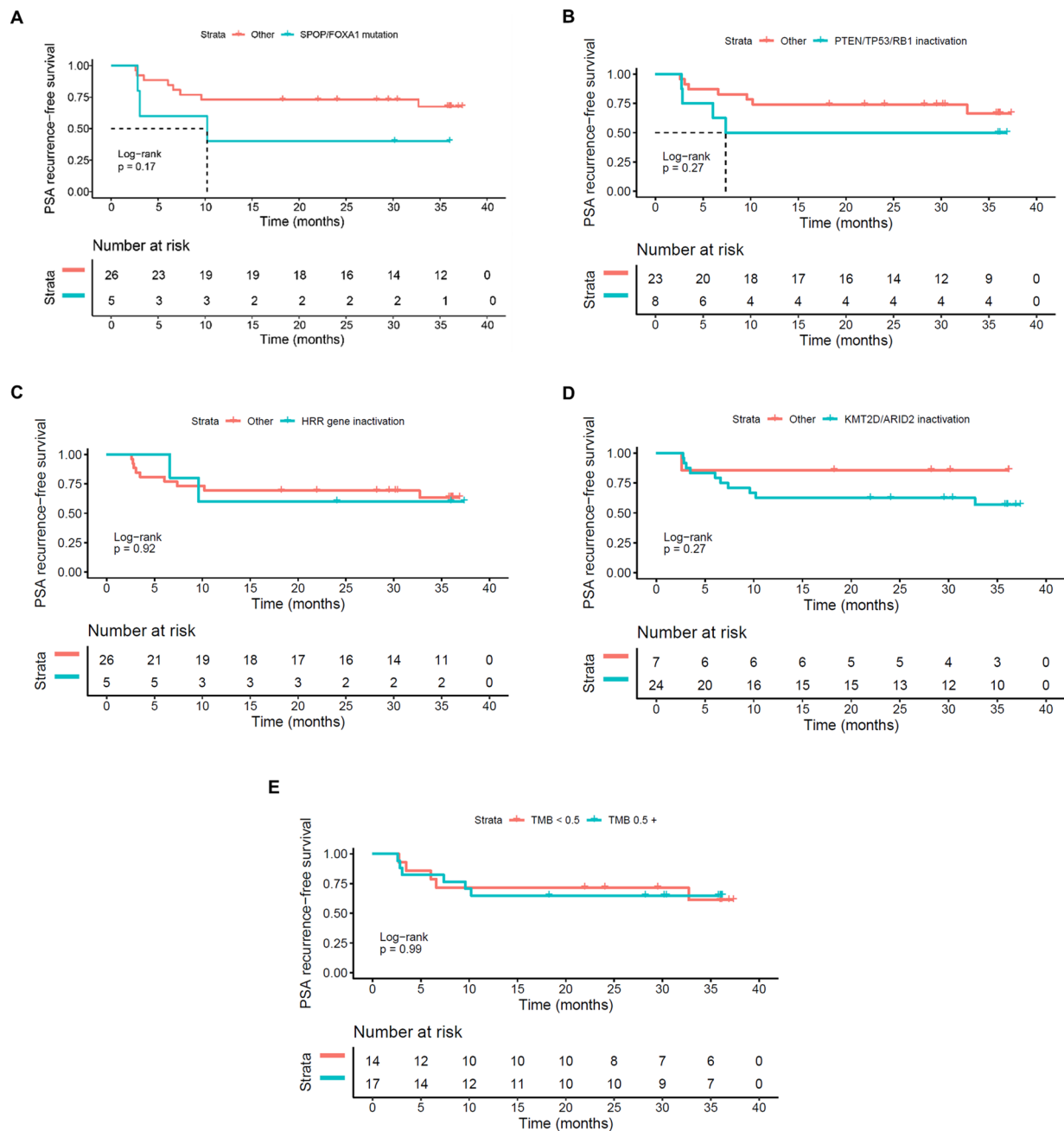
Extended Data Fig. 9 | Kaplan-Meier curves for PSA recurrence-free survival by mutation status post radical prostatectomy. (**a**) *SPOP/FOXA1 mutation:* the median survival was 10.2 months (95% CI: [3.1, NA]) for the *SPOP/FOXA1* mutation group, but it was not reached for the other group, NR months (95% CI: [NR, NR]). The HR of PSA recurrence-free survival for the *SPOP/FOXA1* mutation group compared with the other group is 2.48 (0.65–9.44, p = 0.181). (**b**) *PTEN/ TP53/RB1 inactivation:* the median survival was 7.4 months (95% CI: [6, NR]) for the *PTEN/TP53/RB1* inactivation group, but it was not reached for the other group, NR months (95% CI: [32.7, NR]). The HR of PSA recurrence-free survival for the *PTEN/TP53/RB1* inactivation group compared with the other group is 1.97 (0.57– 6.76, p = 0.281). (**c**) *HRR gene inactivation:* median survival was not reached for both groups, NR months (95% CI: [9.6, NR]) for the HRR gene inactivation group

and NR months (95% CI: [32.7, NR]) for the other group. The HR of PSA recurrence-free survival for the HRR gene inactivation group compared with the other group is 1.08 (0.23–5.01, p = 0.921). (**d**) *KMT2D/ARID2D inactivation:* median survival was not reached for both groups, NR months (95% CI: [10.2, NR]) for the *KMT2D/ ARID2D* inactivation group and NR months (95% CI: [NR, NR]) for the other group. The HR of PSA recurrence-free survival for the *KMT2D/ARID2D* inactivation group compared with the other group is 3.01 (0.38–23.51, p = 0.294). (**e**) *TMB below or above median:* median survival was not reached for both groups, NR months (95% CI: [10.2, NA]) for the TMB 5 mutations/Mb group and NR months (95% CI: [32.7, NR]) for the TMB < 0.5 mutations/Mb group. The HR of PSA recurrence-free survival for the TMB 5 ng/ml group compared with the TMB < 0.5 mutations/Mb group is 1.01 (0.31–3.30, p = 0.990).

Extended Data Table 1 | Pathology outcomes post-treatment

	Overall (N=32)
Gleason grade group at prostatectomy	
2	8 (25.0%)
3	9 (28.1%)
4	0 (0%)
5	15 (46.9%)
Gleason sum at prostatectomy	
7	17 (53.1%)
8	0 (0%)
9 - 10	15 (46.9%)
Pathological (surgical) stage	
Yes	32 (100%)
Presence of lymphovascular invasion	
Yes	2 (6.3%)
No	30 (93.8%)
Presence of extraprostatic extension	
Yes	19 (59.4%)
No	13 (40.6%)
Presence of seminal vesicle invasion	
Yes	8 (25.0%)
No	24 (75.0%)
Positive margins	
Yes	10 (31.3%)
No	22 (68.8%)
Positive lymph nodes	
Yes	4 (12.5%)
No	28 (87.5%)
Pathologic Complete Response (pCR)	
Yes	0 (0%)
No	32 (100%)
CAPRA-S score	
0 - 2	4 (12.5%)
3 - 5	12 (37.5%)
6 +	16 (50.0%)

nature portfolio

Corresponding author(s): Eugene Shenderov

Last updated by author(s): Feb 28, 2023

Reporting Summary

Nature Portfolio wishes to improve the reproducibility of the work that we publish. This form provides structure for consistency and transparency in reporting. For further information on Nature Portfolio policies, see our Editorial Policies and the Editorial Policy Checklist.

Statistics

For all statistical analyses, confirm that the following items are present in the figure legend, table legend, main text, or Methods section.

n/a	Confirmed	
☐	☒	The exact sample size (*n*) for each experimental group/condition, given as a discrete number and unit of measurement
☐	☒	A statement on whether measurements were taken from distinct samples or whether the same sample was measured repeatedly
☐	☒	The statistical test(s) used AND whether they are one- or two-sided *Only common tests should be described solely by name; describe more complex techniques in the Methods section.*
☐	☒	A description of all covariates tested
☐	☒	A description of any assumptions or corrections, such as tests of normality and adjustment for multiple comparisons
☐	☒	A full description of the statistical parameters including central tendency (e.g. means) or other basic estimates (e.g. regression coefficient) AND variation (e.g. standard deviation) or associated estimates of uncertainty (e.g. confidence intervals)
☐	☒	For null hypothesis testing, the test statistic (e.g. *F*, *t*, *r*) with confidence intervals, effect sizes, degrees of freedom and *P* value noted *Give P values as exact values whenever suitable.*
☒	☐	For Bayesian analysis, information on the choice of priors and Markov chain Monte Carlo settings
☒	☐	For hierarchical and complex designs, identification of the appropriate level for tests and full reporting of outcomes
☒	☐	Estimates of effect sizes (e.g. Cohen's *d*, Pearson's *r*), indicating how they were calculated

Our web collection on statistics for biologists contains articles on many of the points above.

Software and code

Policy information about availability of computer code

Data collection	Clinical data was collected in a protected institutional clinical research management system (CRMS).
Data analysis	R Software 4.2.0 and 4.2.2 and lmerTest 3.1-3, Graphpad Prism 9.3.1, GenePix Pro v7.2.30,

For manuscripts utilizing custom algorithms or software that are central to the research but not yet described in published literature, software must be made available to editors and reviewers. We strongly encourage code deposition in a community repository (e.g. GitHub). See the Nature Portfolio guidelines for submitting code & software for further information.

Data

Policy information about availability of data

All manuscripts must include a data availability statement. This statement should provide the following information, where applicable:
- Accession codes, unique identifiers, or web links for publicly available datasets
- A description of any restrictions on data availability
- For clinical datasets or third party data, please ensure that the statement adheres to our policy

TRVB information for 30 patients are available as the project "Neoadjuvant B7H3 Trial in Prostate Cancer" in the immuneACCESS public database: https://clients.adpativebiotech.com/immuneaccess. The study protocol is uploaded as a supplementary file. Authors defer trial participant raw genomic data deposition to national or international public repositories to avoid compromising research participant privacy. A summary of patient whole exome sequence alterations of clinical significance is provided in Supplementary Data Table 4. Aggregate patient-related information has been made available on ClinicalTrials.gov (https://

Human research participants

Policy information about studies involving human research participants and Sex and Gender in Research.

Reporting on sex and gender	32 biological males were enrolled on the study as prostate cancer only occurs in biological males with a prostate organ.
Population characteristics	The 32 patients described in this initial report enrolled in NCT02923180 as per study protocol. The study had a single arm and there was no randomization. Eligible men with histologically confirmed and operable intermediate and high-risk localized PCa (Gleason grade groups 3-5) were enrolled to evaluate the safety, anti-tumor efficacy, and immunogenicity of enoblituzumab when given prior to prostatectomy. Key inclusion criteria included histological adenocarcinoma; clinical stage T1c–T3b, N0, M0; Gleason score 4+3=7 to 5+5=10; at least 2 positive biopsy cores; prior decision to undergo radical prostatectomy; adult male >18 years of age; ECOG performance status 0-1. Key exclusion criteria included prior hormones, biologics, or chemotherapy for prostate cancer; prior immunotherapy/vaccine therapy for prostate cancer; history of autoimmune disease requiring systemic immunosuppression.
Recruitment	This was a single-institution, open-label phase 2 study. Participants were approached during routine clinical visits or at the multi-disciplinary prostate clinic and screened for eligibility/consented if inclusion criteria were met and no exclusion criteria were identified. All patients who met trial criteria were offered the trial without any anticipated bias.
Ethics oversight	Johns Hopkins University Institutional Review Board

Note that full information on the approval of the study protocol must also be provided in the manuscript.

Field-specific reporting

Please select the one below that is the best fit for your research. If you are not sure, read the appropriate sections before making your selection.

☒ Life sciences   ☐ Behavioural & social sciences   ☐ Ecological, evolutionary & environmental sciences

For a reference copy of the document with all sections, see nature.com/documents/nr-reporting-summary-flat.pdf

Life sciences study design

All studies must disclose on these points even when the disclosure is negative.

Sample size	Sample sizes in this study were determined by the original clinical trial design and sample availability.
Data exclusions	No additional inclusion/exclusion criteria were applied beyond the sample sizes determined in the original clinical trial design and sample availability.
Replication	Genomic analysis was performed once per biological patient sample due to expense of sequencing and tumor sample availability. ELISA experiments were performed once with duplicate wells per biological patient sample. Replications were consistent. DSP and IO360 analyses were performed once per biological sample due to expense and sample availability. Per each DSP patient sample multiple ROIs were selected.
Randomization	The clinical trial herein was a single-treatment study. Comparisons were intrapatient (biopsy versus prostatectomy), responders versus non-responder, and utilizing a 1:1 matched historical cohort.
Blinding	The clinical trial was not blinded as per study design and was not placebo controlled. Pathology assessment was done in a blinded manner and correlative assays were conducted using de-identified subject samples.

Reporting for specific materials, systems and methods

We require information from authors about some types of materials, experimental systems and methods used in many studies. Here, indicate whether each material, system or method listed is relevant to your study. If you are not sure if a list item applies to your research, read the appropriate section before selecting a response.

Materials & experimental systems

n/a	Involved in the study
☐	☒ Antibodies
☒	☐ Eukaryotic cell lines
☒	☐ Palaeontology and archaeology
☒	☐ Animals and other organisms
☐	☒ Clinical data
☒	☐ Dual use research of concern

Methods

n/a	Involved in the study
☒	☐ ChIP-seq
☒	☐ Flow cytometry
☒	☐ MRI-based neuroimaging

Antibodies

Antibodies used	Enoblituzumab (Macrogenics, Inc). Commercially available rabbit anti-human B7-H3 mAb (clone SP206, Spring Biosciences, catalog no. M5064.C, 0.2 ug/mL), hCD68 Alexa Fluor 647 (clone KP1, Santa Cruz, catalog no. sc-20060 AF647, 1.4 ug/mL), hCD3 conjugated to Alexa Fluor 594 (clone UMAB54, Origene, 3.6 ug/mL), hCK8/18 Alexa Fluor 532 (clone K8.8+DC10, Novus, catalog no. NBP2-34655AF532, 2.3 ug/mL), hIgG Fc gamma fragment specific Alexa Fluor 647 (polyclonal, Jackson ImmunoResearch, catalog no. 109-606-098, 0.25 ug/mL), hIgM Fc5u fragment specific Cy3 (polyclonal, Jackson ImmunoResearch, catalog no. 109-165-043, 0.25 ug/mL).
Validation	Commercially available antibodies as validated by manufacturer were utilized.

Clinical data

Policy information about clinical studies

All manuscripts should comply with the ICMJE guidelines for publication of clinical research and a completed CONSORT checklist must be included with all submissions.

Clinical trial registration	NCT02923180
Study protocol	The full trial protocol will be made available as part of the supplemental material
Data collection	Clinical data was collected at The Johns Hopkins Hospital, the single site of the clinical trial NCT02923180. All data was collected between February 14, 2017 through June 10, 2019.
Outcomes	Primary Endpoints: 1) To confirm the safety and feasibility of Enoblituzumab administered using a standard dose / schedule in the neo-adjuvant setting 2) PSA0 Response (Undetectable PSA level <0.1 ng/mL) at 12 months following radical prostatectomy Secondary Endpoints: 1) To quantify an anti-tumor response to Enoblituzumab 2) To assess the immune response to Enoblituzumab 3) To assess Gleason grade change post neoadjuvant Enoblituzumab treatment, by comparing prostatectomy Gleason sum to pre-treatment biopsy Gleason sum 4) To quantify the extent of PD-L1+ cell density in the prostate from harvested prostate glands of treated patients. 5) To quantify the NK cell density in tumor tissue from harvested prostate glands of patients 6) To quantify tissue androgen concentration (testosterone, dihydrotestosterone) and androgen receptor (AR) protein expression in prostate specimens Assessment: Patient on-treatment visits occurred on days 1, 8, 15, 22, 29, 36) (±1 day). At each visit safety evaluation was completed for frequency, types, and grades of adverse events measured using the NCI Common Toxicity Criteria version 4.0. Safety assessment was performed on the day of radical prostatectomy (Da6 50 +/- 3 days) and on follow up evaluation visits 30 and 90 days after radical prostatectomy.